Introduction to Saturation Physics

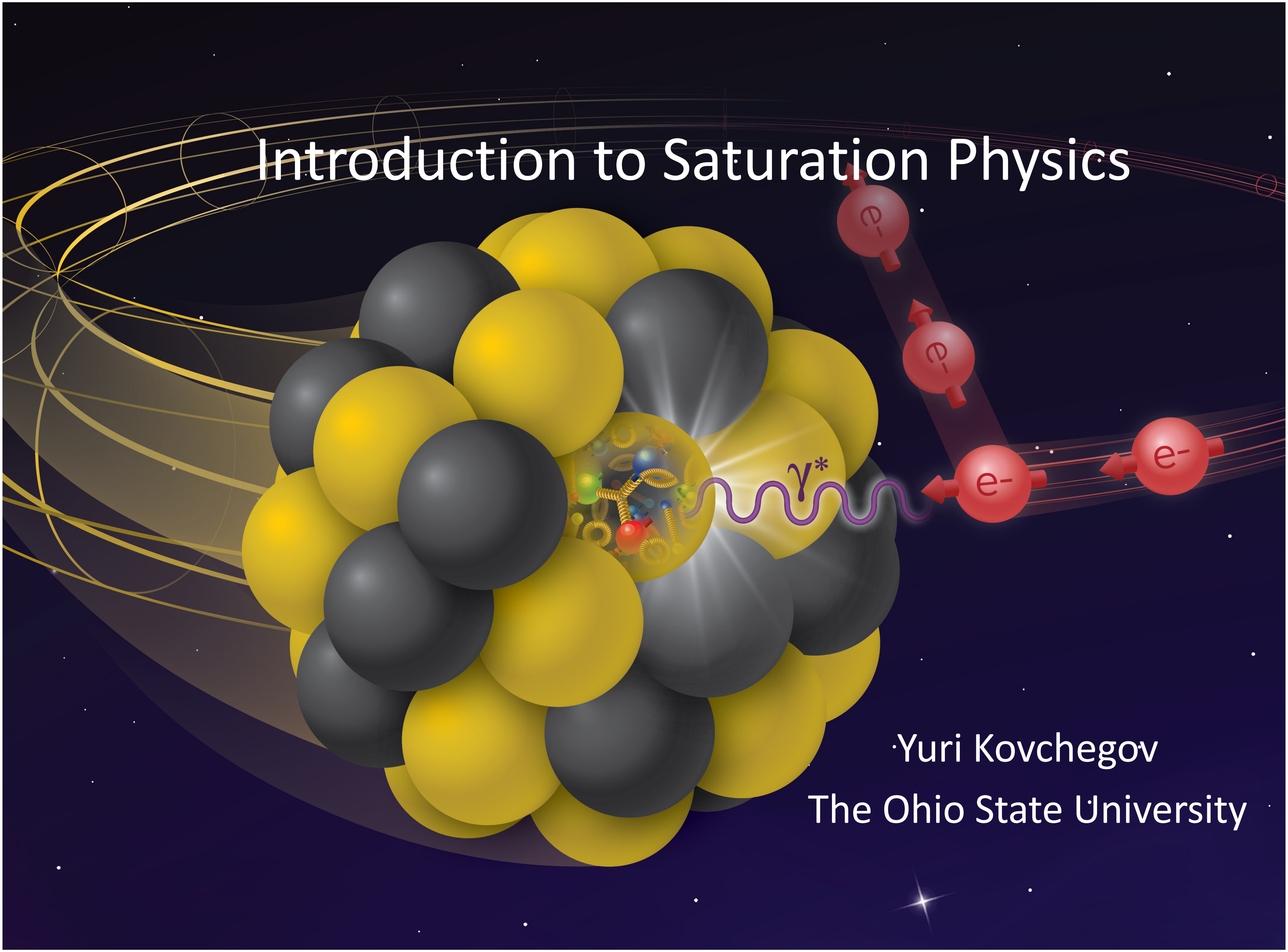

Yuri Kovchegov
The Ohio State University

Outline

- Classical small-*x* physics:
  - DIS in the dipole picture, Glauber-Gribov-Mueller formula
  - Black disk limit, parton saturation, saturation scale
  - McLerran-Venugopalan model, saturation scale for a nucleus
- Nonlinear small-*x* evolution:
  - Non-linear BK and JIMWLK evolution equations
  - Solution of BK and JIMWLK equations, unitarity, energy dependence of the saturation scale
  - Map of high-energy QCD
- Saturation physics at the future Electron-Ion Collider (EIC)
  - Brief history of EIC (to this point)
  - Searches for saturation physics at EIC: structure functions, di-hadron correlations, diffraction
- Conclusions

Quasi-classical approximation

Kinematics of DIS

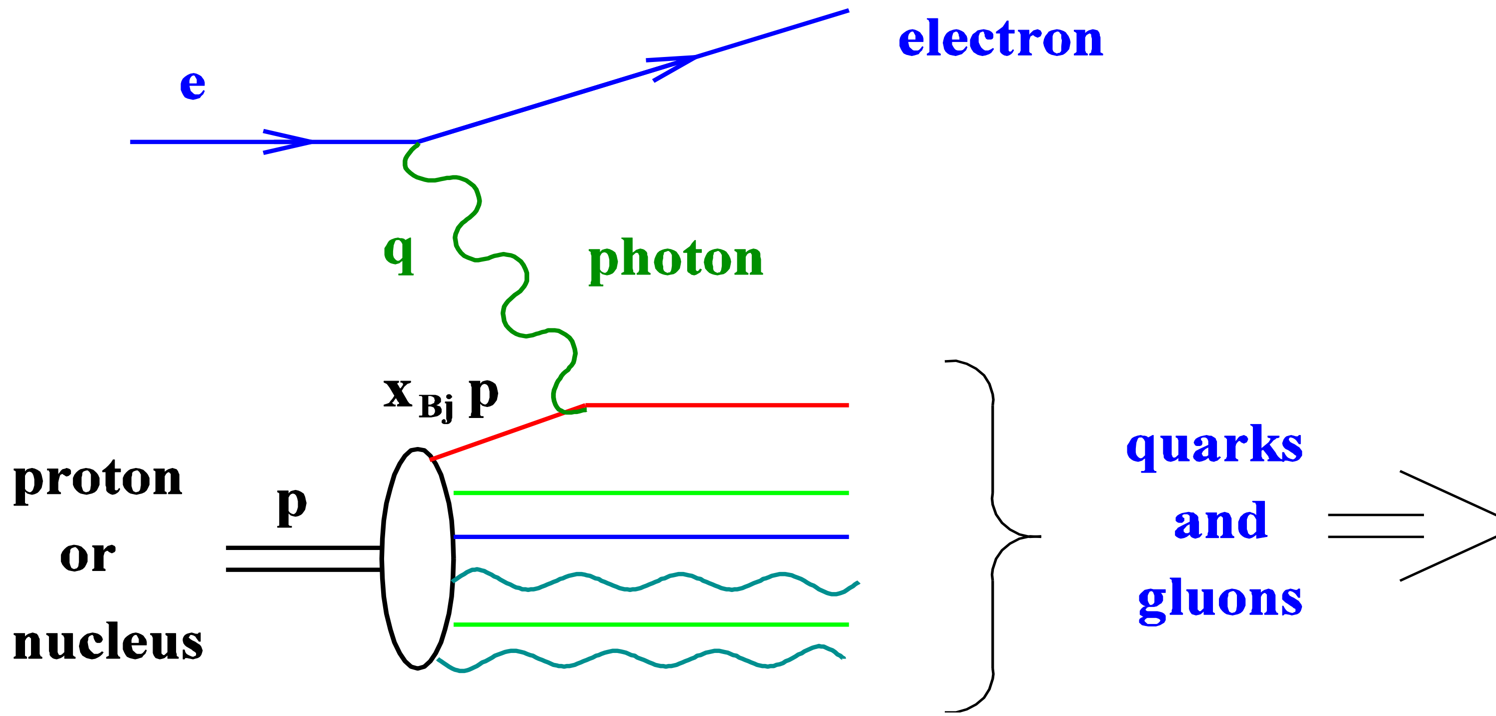

- Photon carries 4-momentum q_μ , its virtuality is

$$Q^2 = -q_\mu \, q^\mu$$

- Photon hits a quark in the proton carrying momentum $x_{Bj}\,p$ with p being the proton's momentum. Parameter x_{Bj} is the Bjorken *x* variable.

Dipole picture of DIS

- At small x, the dominant contribution to DIS structure functions does not come from the handbag diagram.

- Instead, the dominant terms comes from the dipole picture of DIS, where the virtual photon splits into a quark-antiquark pair, which then interacts with the target.

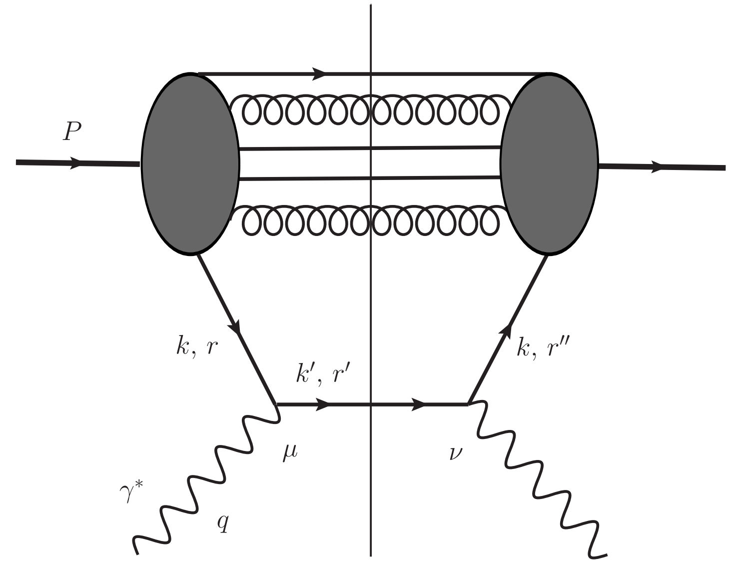

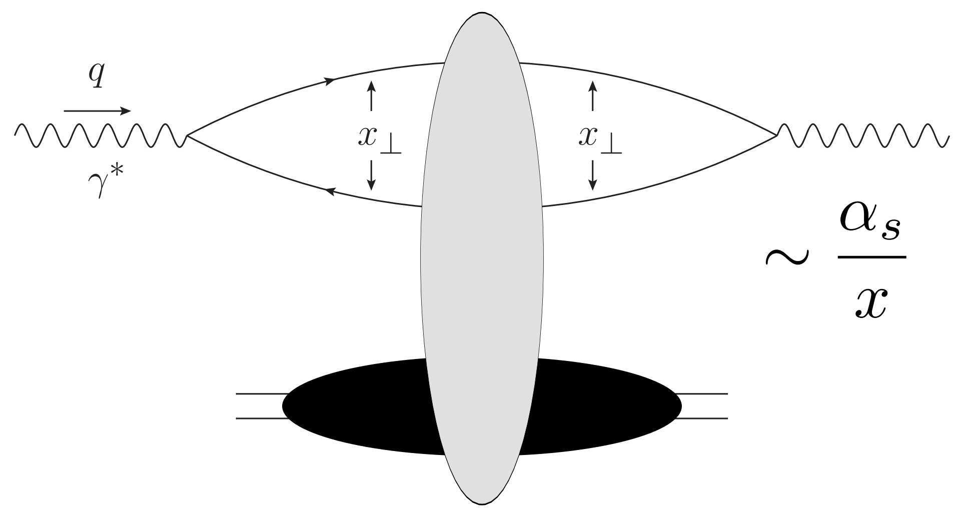

$$\sim \frac{\alpha_s}{x}$$

Dipole Amplitude

- The total DIS cross section is expressed in terms of the (Im part of the) forward quark dipole amplitude N:

$$\sigma_{tot}^{\gamma^* A} = \int \frac{d^2 x_\perp}{2\,\pi}\, d^2 b_\perp \int_0^1 \frac{dz}{z\,(1-z)}\; |\Psi^{\gamma^* \to q\bar{q}}(\vec{x}_\perp, z)|^2 \; N(\vec{x}_\perp, \vec{b}_\perp, Y)$$

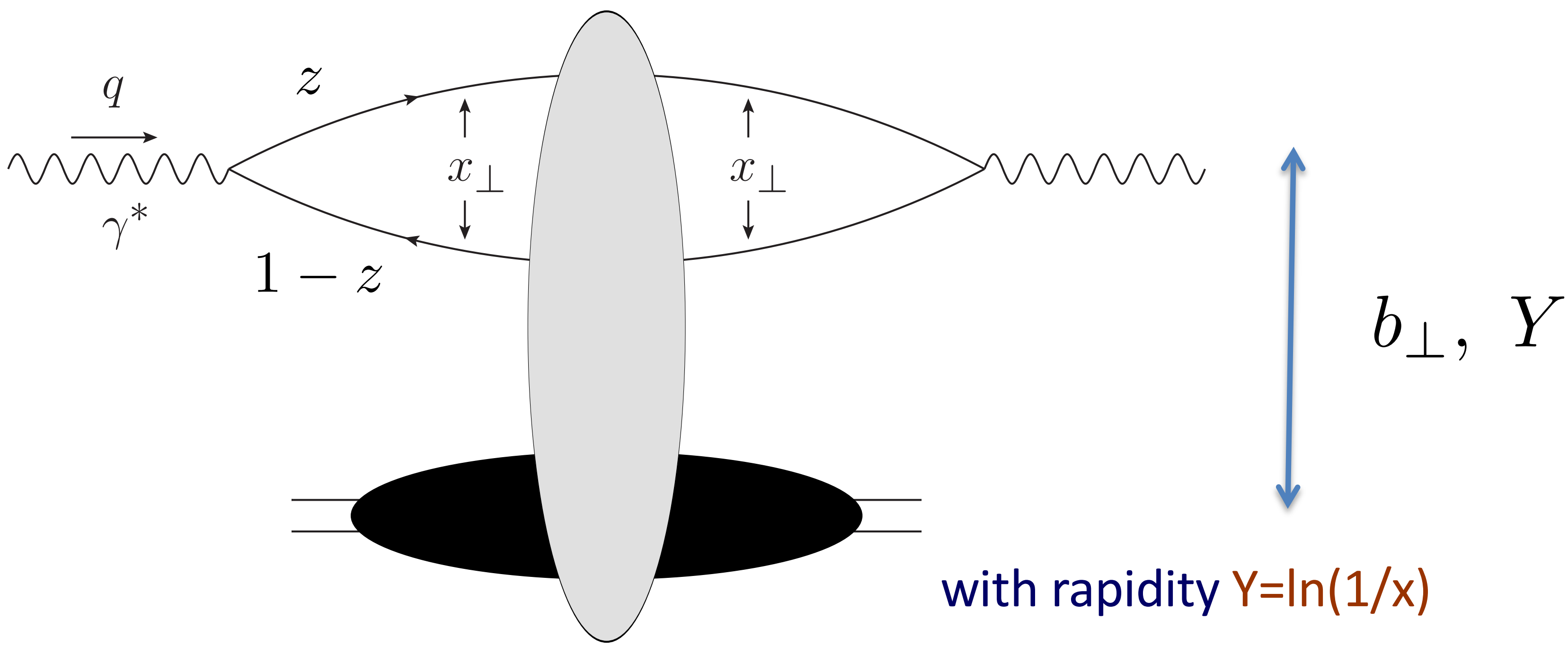

with rapidity Y=ln(1/x)

DIS in the Classical Approximation

The DIS process in the rest frame of the target nucleus is shown below.

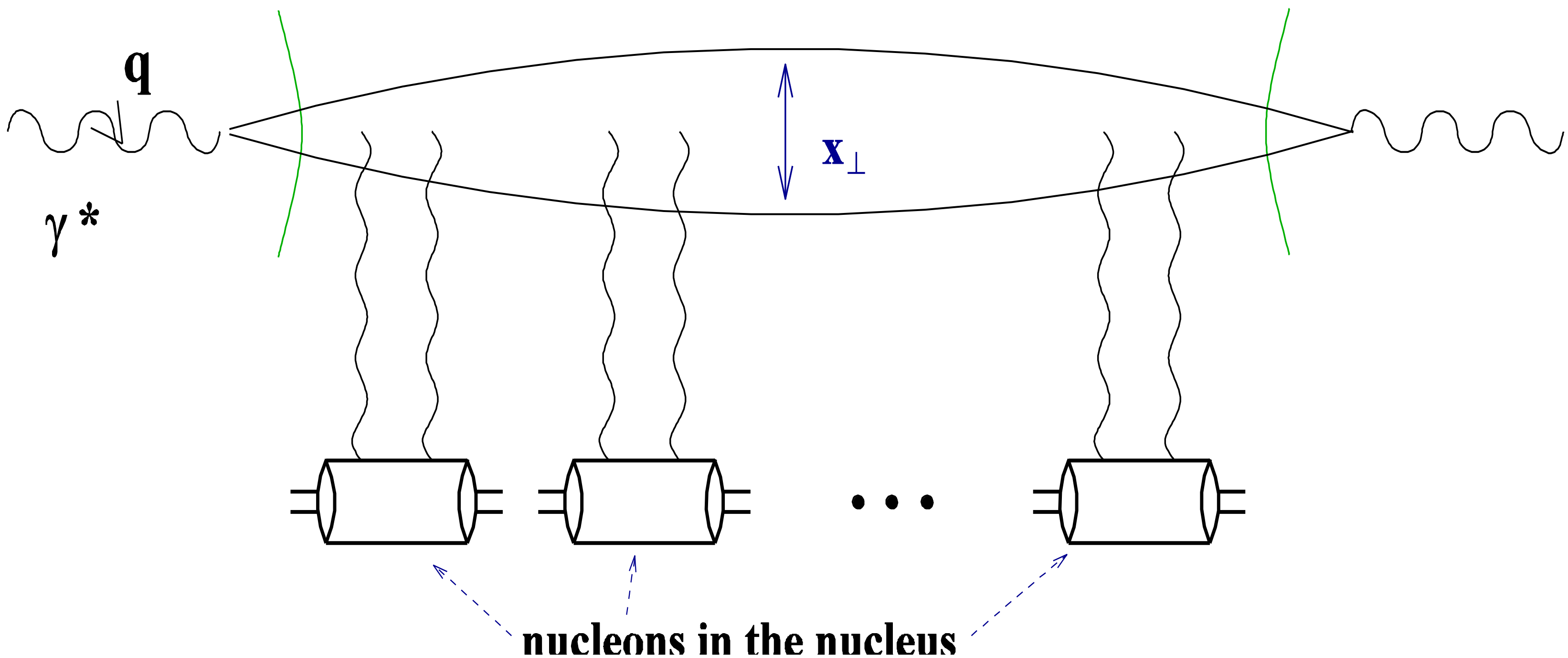

$$\sigma_{tot}^{\gamma^* A}(x_{Bj}, Q^2) = |\Psi^{\gamma^*\to q\bar{q}}|^2 \otimes N(x_\perp, Y = \ln 1/x_{Bj})$$

with rapidity Y=ln(1/x)

Dipole Amplitude

- The quark dipole amplitude is defined by

$$N(\underline{x}_1, \underline{x}_2) = 1 - \frac{1}{N_c} \left\langle \mathrm{tr} \left[V(\underline{x}_1)\, V^\dagger(\underline{x}_2) \right] \right\rangle$$

- Here we use the Wilson lines along the light-cone direction

$$V(\underline{x}) = \mathrm{P} \exp \left[i\, g \int\limits_{-\infty}^{\infty} dx^+ \, A^-(x^+, x^- = 0, \underline{x}) \right]$$

- In the classical Glauber-Mueller/McLerran-Venugopalan approach the dipole amplitude resums multiple rescatterings:

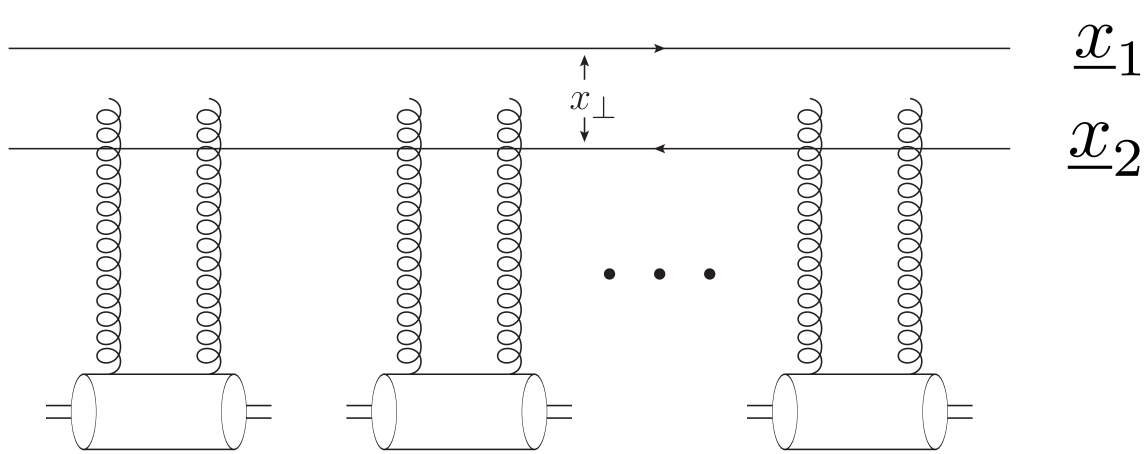

Quasi-classical dipole amplitude

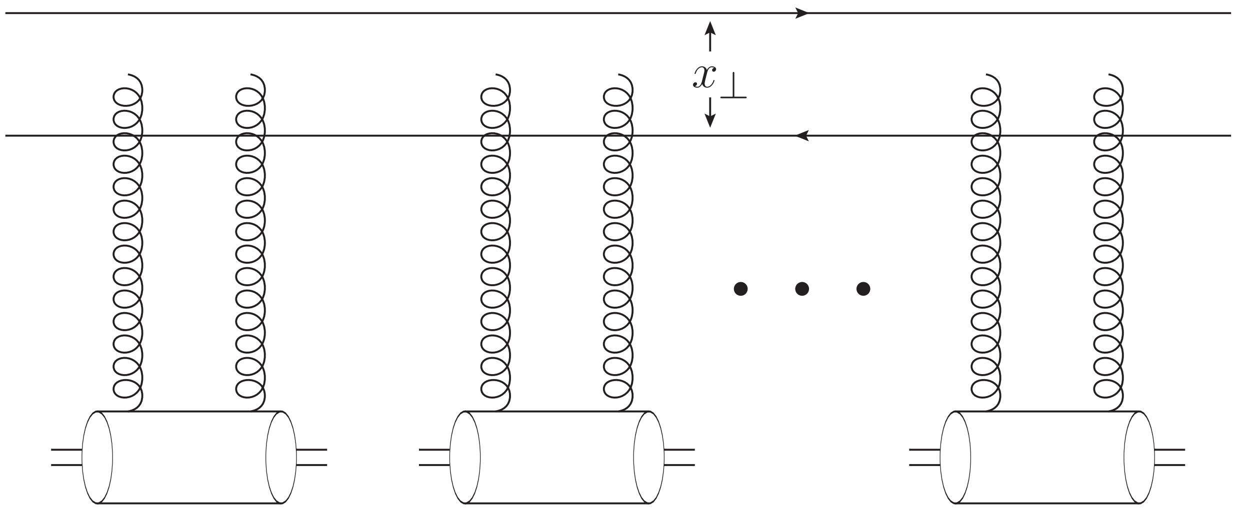

A.H. Mueller, '90

Lowest-order interaction with each nucleon – two gluon exchange – the same resummation parameter as in the MV model: $\alpha_s^2\, A^{1/3}$

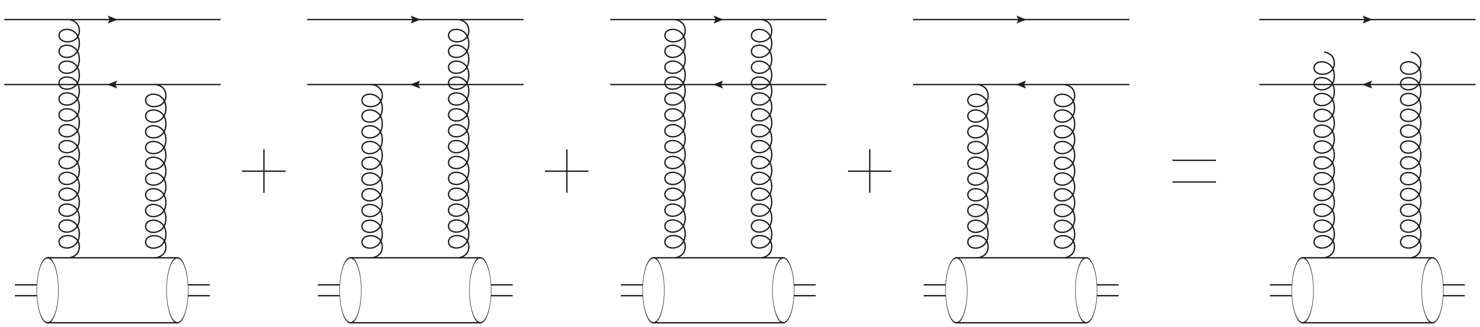

Quasi-classical dipole amplitude

- To resum multiple rescatterings, note that the nucleons are independent of each other and rescatterings on the nucleons are also independent.

- One then writes an equation (Mueller '90)

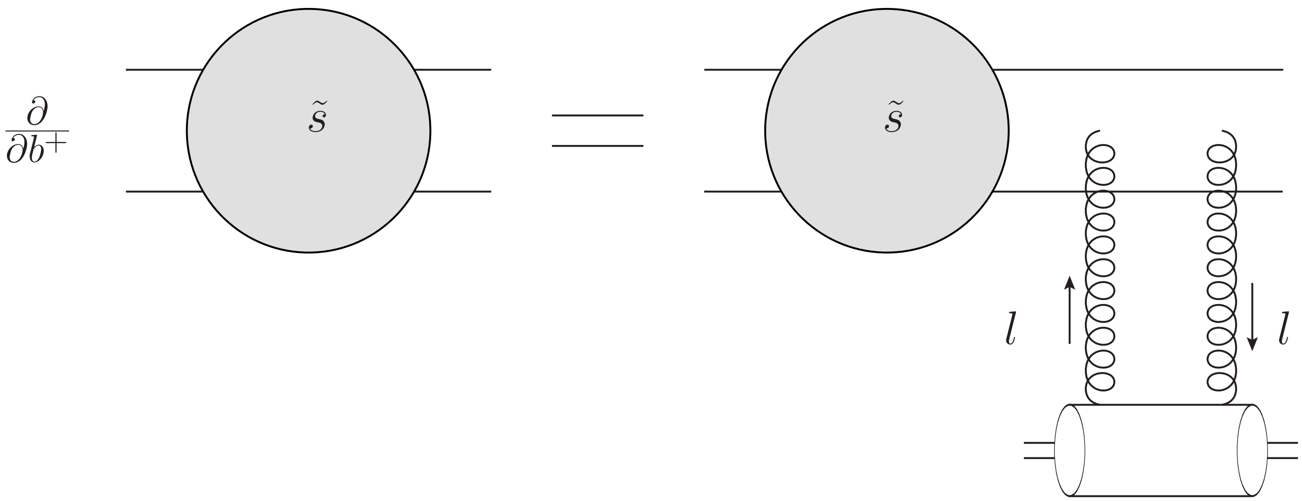

Each scattering!

$$N(x_\perp, Y) = 1 - \exp\left[-\frac{x_\perp^2 Q_s^2}{4} \ln \frac{1}{x_\perp \Lambda} \right]$$

DIS in the Classical Approximation

The dipole-nucleus amplitude in the classical approximation is

$$\sigma^{q\bar{q}A} = 2 \int d^2b\, N(x_\perp, b_\perp, Y)$$

$$N(x_\perp, Y) = 1 - \exp\left[-\frac{x_\perp^2\, Q_s^2}{4}\, \ln \frac{1}{x_\perp\, \Lambda} \right]$$

A.H. Mueller, ‘90

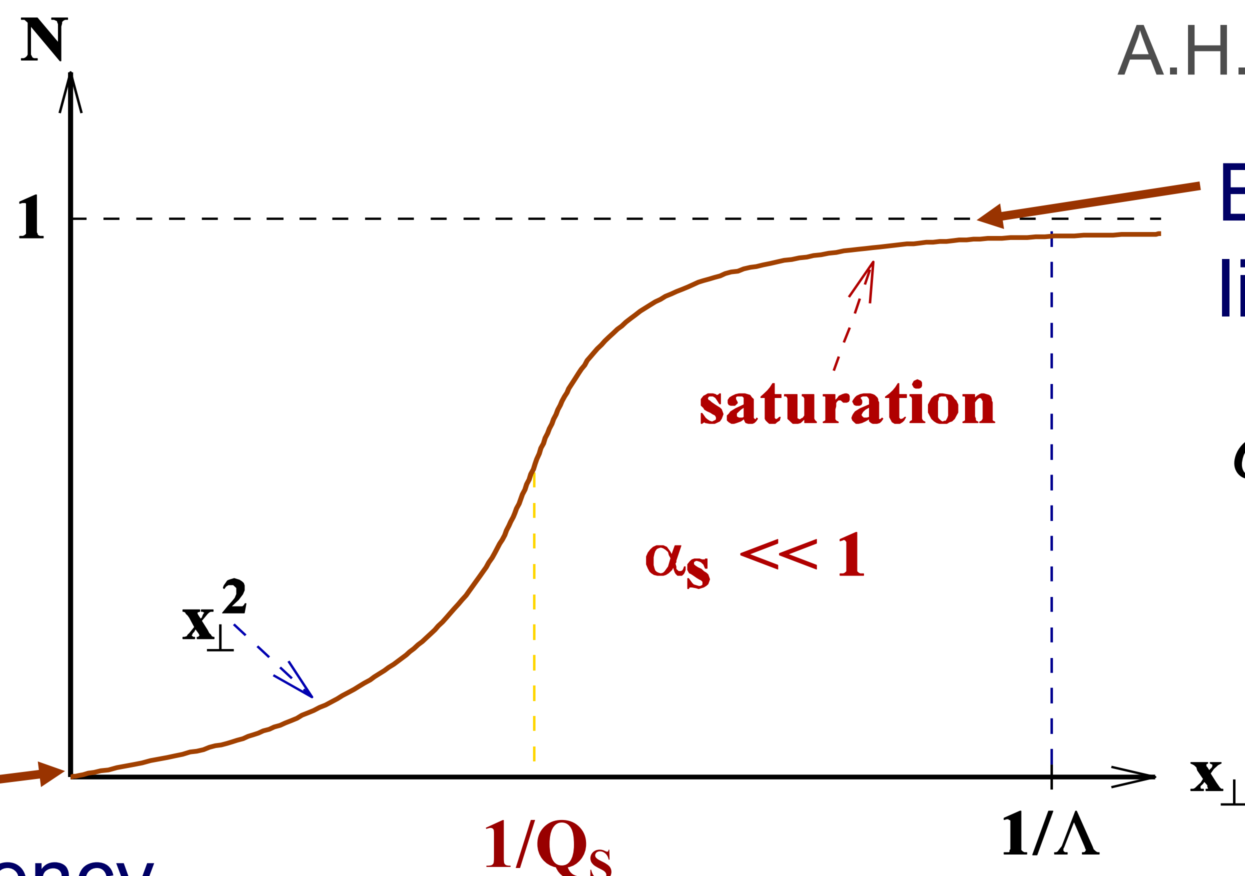

Black disk limit,

$$\sigma_{tot} < 2\pi R^2$$

Color transparency

$$Q_S^2 \sim A^{1/3}$$

McLerran-Venugopalan Model

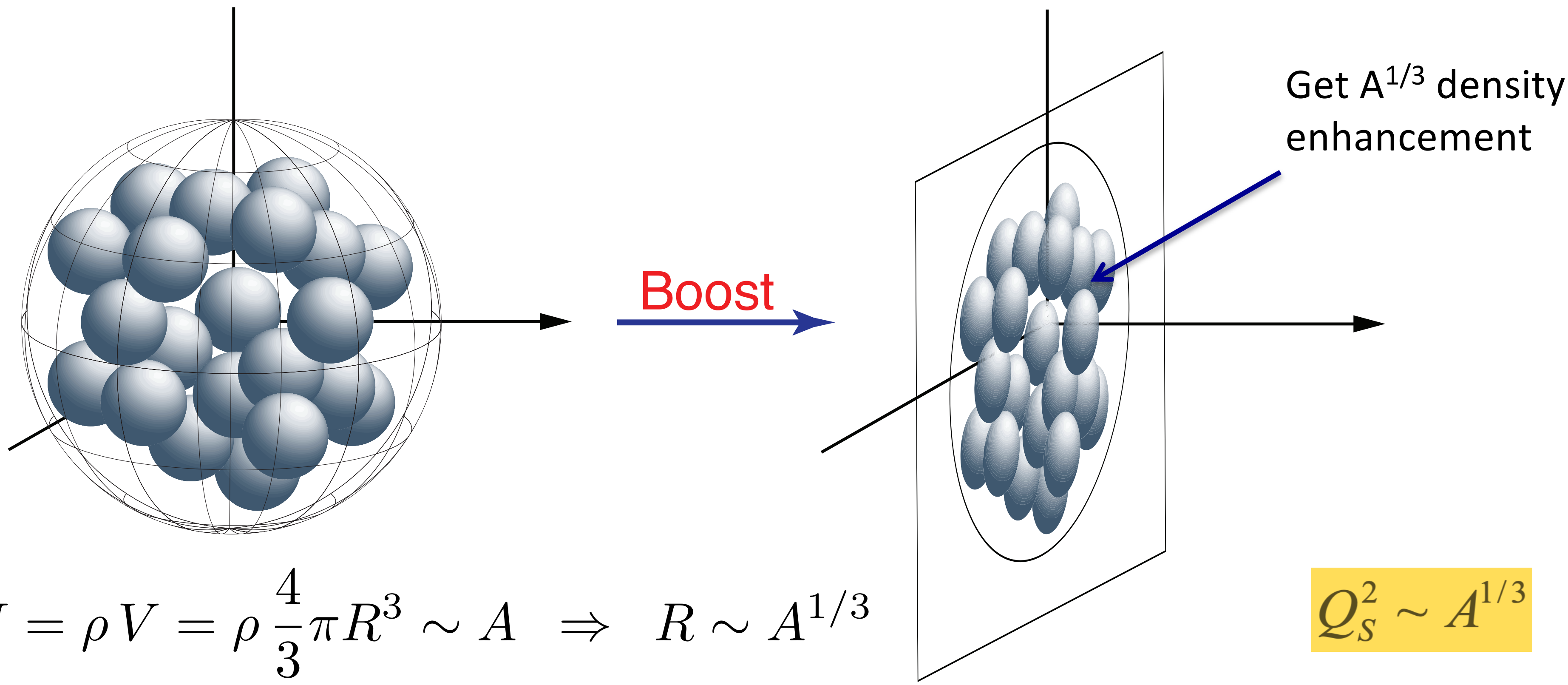

$$M = \rho V = \rho \frac{4}{3}\pi R^3 \sim A \quad \Rightarrow \quad R \sim A^{1/3}$$

$$Q_S^2 \sim A^{1/3}$$

- Large gluon density gives a large momentum scale Q_s (the saturation scale): Q_s^2 ~ # gluons per unit transverse area ~ $A^{1/3}$ (nuclear oomph).
- For $Q_s >> \Lambda_{QCD}$, get a theory at weak coupling $\alpha_s(Q_s^2) \ll 1$ and the leading gluon field is <u>classical</u>.

Small-x evolution equations

Quantum Evolution

- The energy dependence comes in through the long-lived s-channel gluon corrections (higher Fock states):

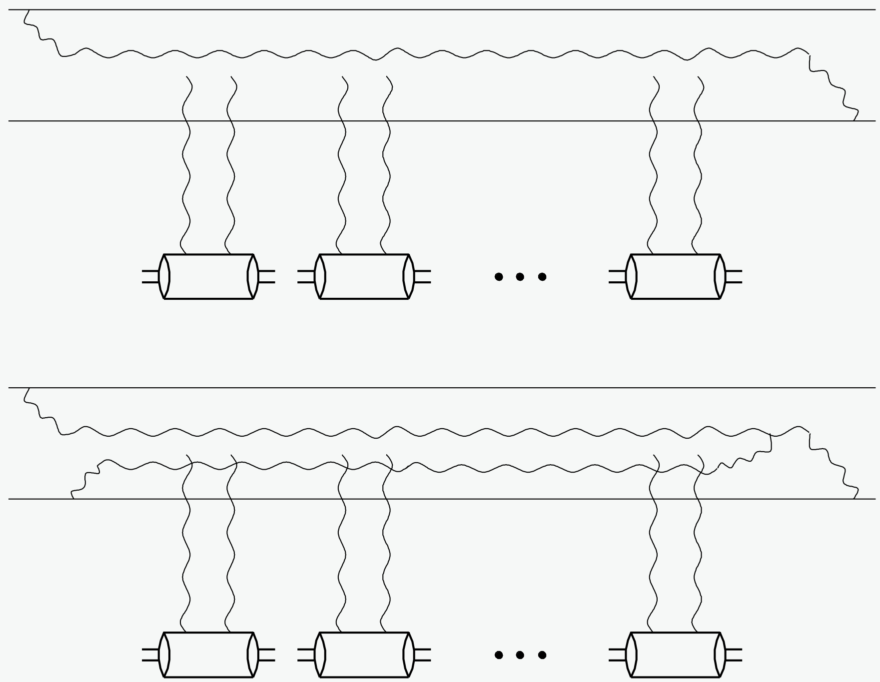

$$\alpha_s \ln s \sim \alpha_s Y \sim 1$$

These extra gluons bring in powers of α_S ln s, such that when α_S << 1 and ln s >>1 this parameter is α_S ln s ~ 1 (leading logarithmic approximation, LLA).

Mueller's Dipole Model

To include the quantum evolution in a dipole amplitude one can use the approach developed by A. H. Mueller in '93-'94.

Emission of a small-x gluon taken in the large-N_C limit would split the original color dipole in two:

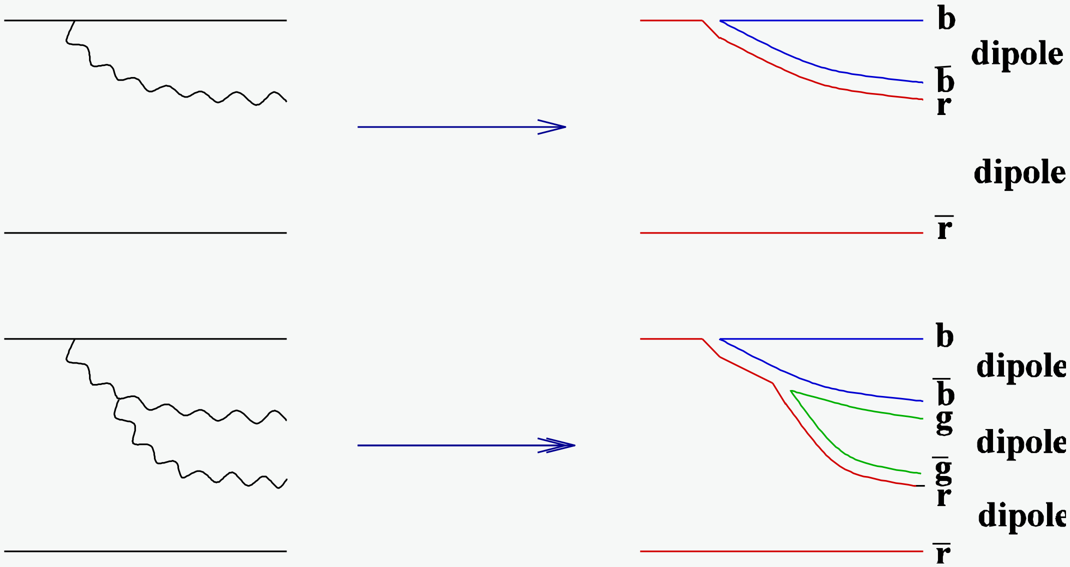

$$3 \otimes \bar{3} = 1 \oplus 8 \quad \Rightarrow \quad N_c \otimes \bar{N}_c = 1 \oplus (N_c^2 - 1) \approx N_c^2 - 1$$

Re-summing gluon cascade

- At large N_c the gluon cascade turns into a dipole cascade. We need to resum the dipole cascade, with each dipole interacting with the target independently.

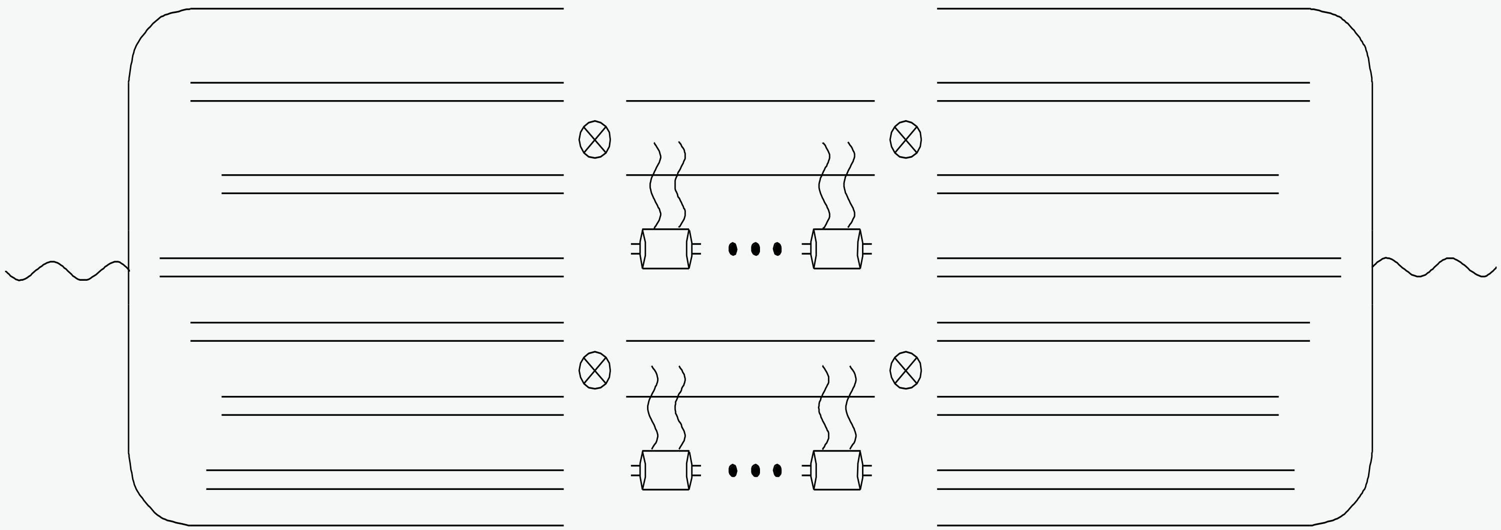

Notation (Large-N_c)

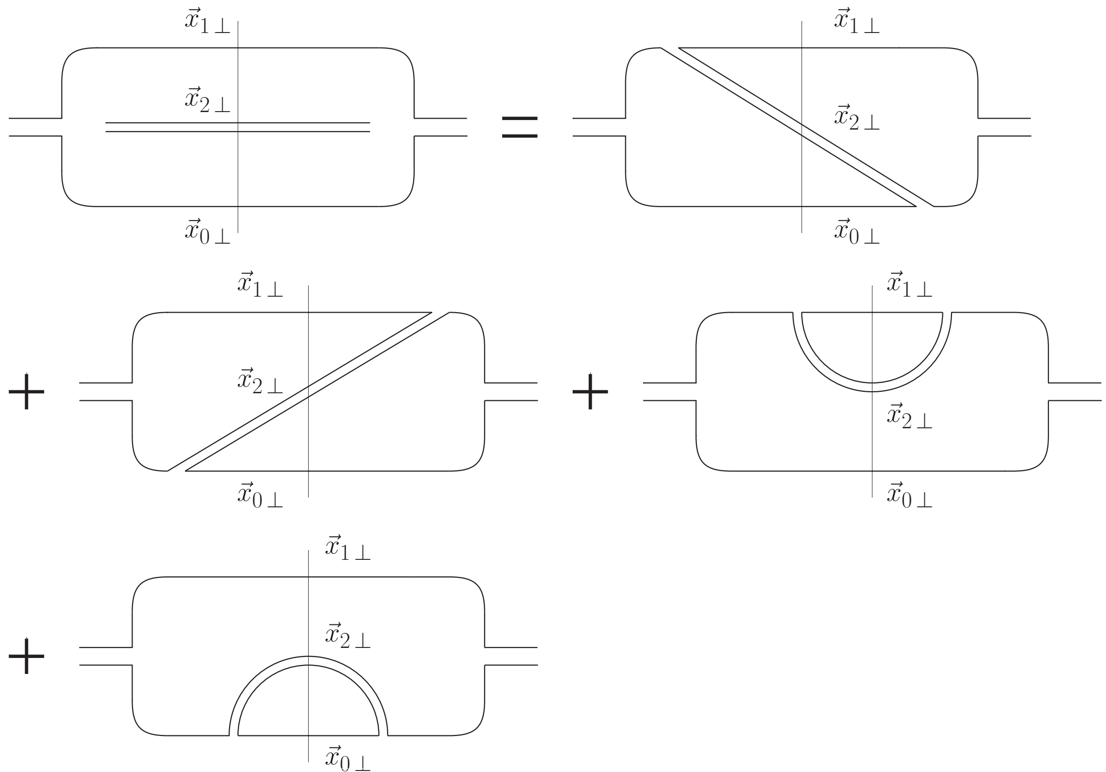

Real emissions in the amplitude squared

(dashed line – all Glauber-Mueller exchanges at light-cone time =0)

Virtual corrections in the amplitude (wave function)

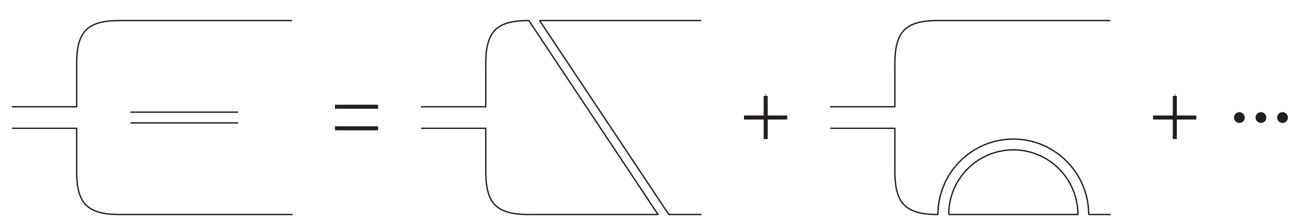

Nonlinear Evolution

To sum up the gluon cascade at large-N_C we write the following equation for the dipole S-matrix:

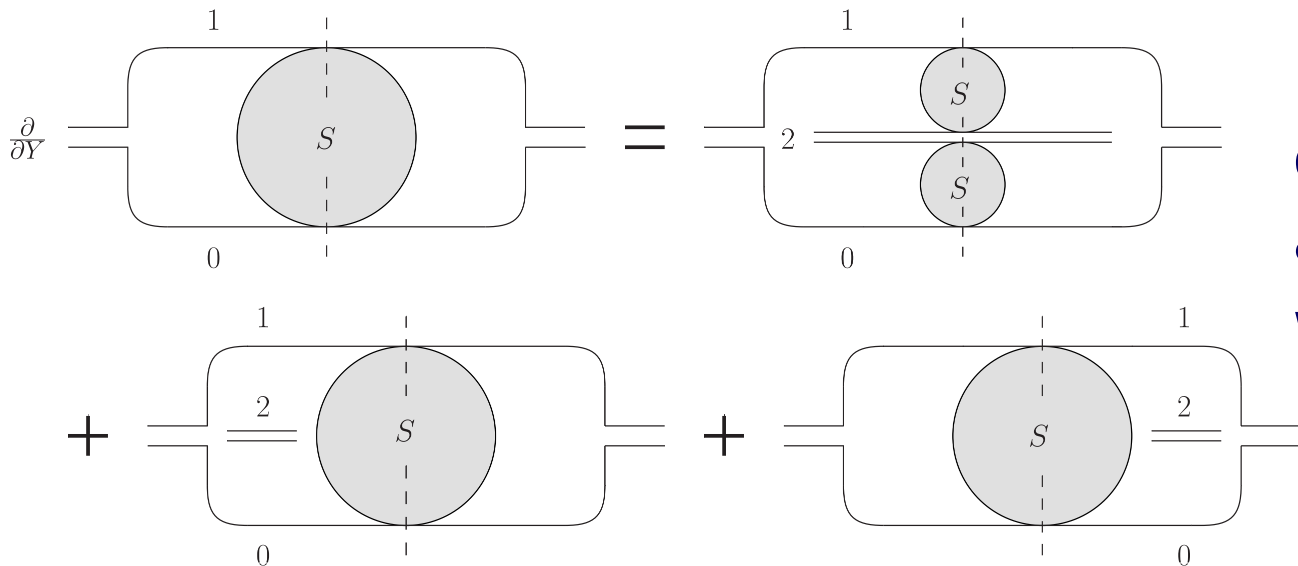

dashed line = all interactions with the target

$$\partial_Y S_{\mathbf{x}_0,\mathbf{x}_1}(Y) = \frac{\alpha_s N_c}{2\pi^2} \int d^2 x_2 \frac{x_{01}^2}{x_{02}^2 x_{21}^2} \left[S_{\mathbf{x}_0,\mathbf{x}_2}(Y) S_{\mathbf{x}_2,\mathbf{x}_1}(Y) - S_{\mathbf{x}_0,\mathbf{x}_1}(Y) \right]$$

Remembering that S= 1-N we can rewrite this equation in terms of the dipole scattering amplitude N.

Nonlinear evolution at large N_c

As N=1-S we write

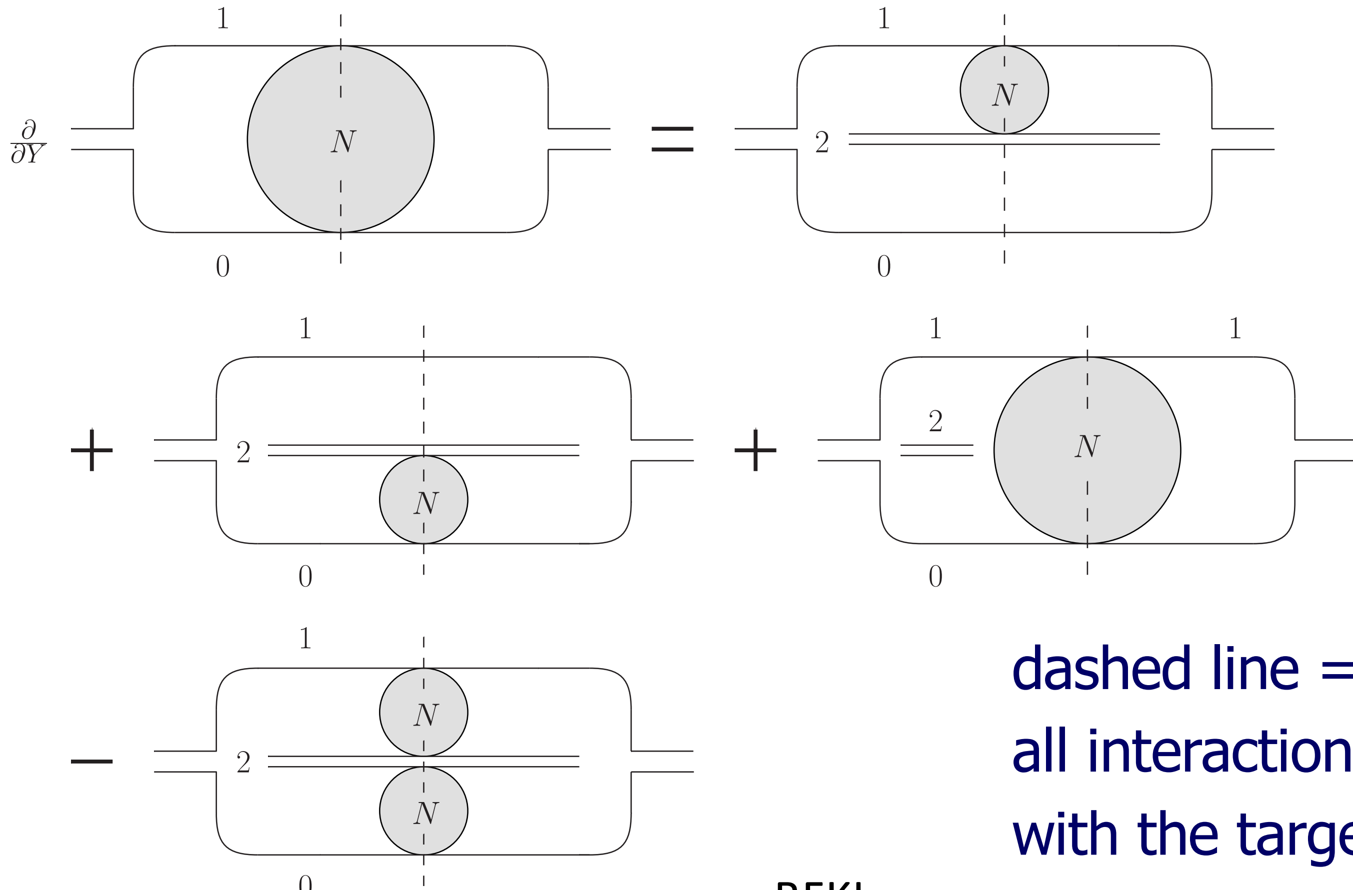

dashed line =
all interactions
with the target

$$\partial_Y N_{\mathbf{x}_0,\mathbf{x}_1}(Y) = \frac{\alpha_s N_c}{2\pi^2} \int d^2 x_2 \, \frac{x_{01}^2}{x_{02}^2 \, x_{21}^2} \, [\overbrace{N_{\mathbf{x}_0,\mathbf{x}_2}(Y) + N_{\mathbf{x}_2,\mathbf{x}_1}(Y) - N_{\mathbf{x}_0,\mathbf{x}_1}(Y)}^{\text{BFKL}} - N_{\mathbf{x}_0,\mathbf{x}_2}(Y) \, N_{\mathbf{x}_2,\mathbf{x}_1}(Y)]$$

Balitsky ‘96, Yu.K. ‘99

Nonlinear Evolution Equation

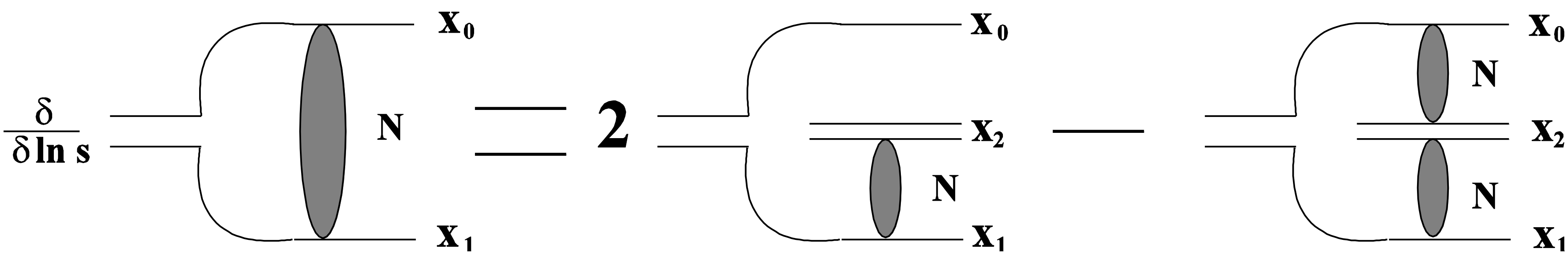

We can resum the dipole cascade

$$\frac{\partial N(x_{01},Y)}{\partial Y} = \frac{\alpha_S N_C}{\pi^2}\int d^2x_2 \left[\frac{x_{01}^2}{x_{02}^2\, x_{12}^2} - 2\pi\,\delta^2(\underline{x}_{01}-\underline{x}_{02})\ln\left(\frac{x_{01}}{\rho}\right)\right] N(x_{02},Y)$$

$$-\frac{\alpha_S N_C}{2\pi^2}\int d^2x_2\, \frac{x_{01}^2}{x_{02}^2\, x_{12}^2} N(x_{02},Y)\, N(x_{12},Y)$$

I. Balitsky, ’96, HE effective lagrangian
Yu. K., ’99, large N_C QCD

$$N(x_\perp, Y) = 1 - \exp\left[-\frac{x_\perp^2\, Q_s^2}{4}\ \ln\frac{1}{x_\perp\,\Lambda}\right]$$

initial condition

⇨ Linear part is BFKL, quadratic term brings in damping

Resummation parameter

- BK equation resums powers of

$$\alpha_s \, N_c \, Y$$

- The Galuber-Mueller/McLerran-Venugopalan initial conditions for it resum powers of

$$\alpha_s^2 \, A^{1/3}$$

JIMWLK: derivation outline

A.H. Mueller, 2001

- Start by introducing a weight functional, $W_Y[\alpha]$. Here $\alpha = A^+$ is the gluon field of the target proton or nucleus. $\alpha(x^-, \vec{x}) \equiv A^+(x^+ = 0, x^-, \vec{x})$
- The functional is used to generate expectation values of gluon-field dependent operators in the target state:

$$\langle \hat{O}_\alpha \rangle_Y = \int \mathcal{D}\alpha \; \hat{O}_\alpha \, W_Y[\alpha]$$

- Imagine that we know small-x evolution for some operator O:

$$\partial_Y \, \langle \hat{O}_\alpha \rangle_Y = \langle \mathcal{K}_\alpha \otimes \hat{O}_\alpha \rangle_Y = \int \mathcal{D}\alpha \, \left[\mathcal{K}_\alpha \otimes \hat{O}_\alpha \right] \, W_Y[\alpha]$$

- On the other hand, we can differentiate the first equation above,

$$\partial_Y \, \langle \hat{O}_\alpha \rangle_Y = \int \mathcal{D}\alpha \; \hat{O}_\alpha \; \partial_Y \, W_Y[\alpha]$$

- Comparing the last two equations and integrating by parts in the second to last equation, we will arrive at and equation for the weight functional $W_Y[\alpha]$.

JIMWLK: derivation outline

- As a test operator, take a pair of Wilson lines (not a dipole!):

$$\hat{O}_{\vec{x}_{1\perp},\vec{x}_{0\perp}} = V_{\vec{x}_{1\perp}} \otimes V^{\dagger}_{\vec{x}_{0\perp}}$$

- Construct the evolution of this operator by summing the following familiar diagrams:

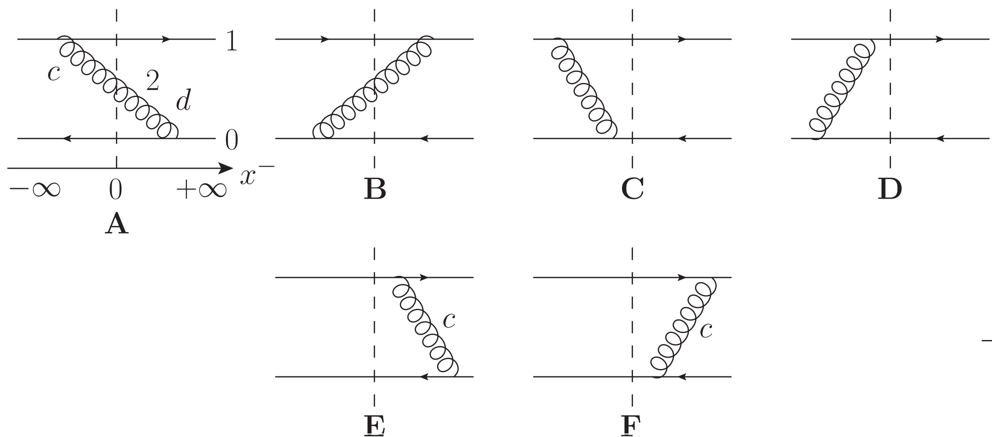

real

virtual

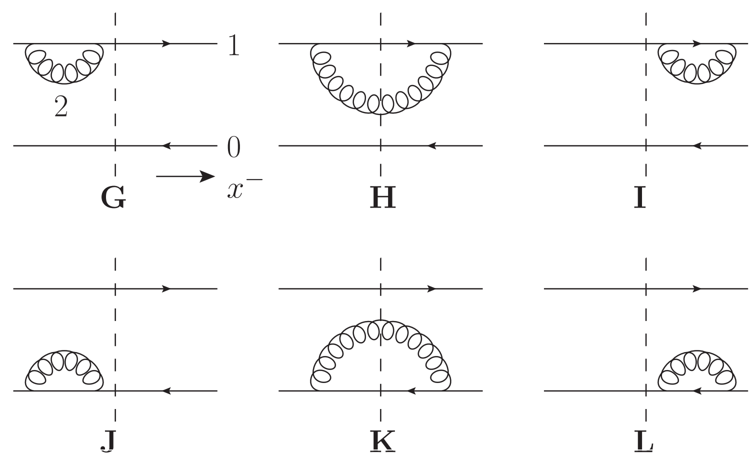

JIMWLK Equation

- In the end one arrive at the JIMWLK evolution equation (1997-2002):

$$\partial_Y W_Y[\alpha] = \alpha_s \left\{ \frac{1}{2} \int d^2x_\perp \, d^2y_\perp \, \frac{\delta^2}{\delta\alpha^a(x^-, \vec{x}_\perp) \, \delta\alpha^b(y^-, \vec{y}_\perp)} \, \left[\eta^{ab}_{\vec{x}_\perp \vec{y}_\perp} W_Y[\alpha] \right] \right.$$
$$\left. - \int d^2x_\perp \, \frac{\delta}{\delta\alpha^a(x^-, \vec{x}_\perp)} \, \left[\nu^a_{\vec{x}_\perp} W_Y[\alpha] \right] \right\}$$

with

$$\eta^{ab}_{\vec{x}_{1\perp} \vec{x}_{0\perp}} = \frac{4}{g^2 \, \pi^2} \int d^2x_2 \, \frac{\vec{x}_{21} \cdot \vec{x}_{20}}{x_{21}^2 \, x_{20}^2} \, \left[\mathbf{1} - U_{\vec{x}_{1\perp}} U^\dagger_{\vec{x}_{2\perp}} - U_{\vec{x}_{2\perp}} U^\dagger_{\vec{x}_{0\perp}} + U_{\vec{x}_{1\perp}} U^\dagger_{\vec{x}_{0\perp}} \right]^{ab}$$

$$\nu^a_{\vec{x}_{1\perp}} = \frac{i}{g \, \pi^2} \int \frac{d^2x_2}{x_{21}^2} \, \mathrm{Tr} \left[T^a U_{\vec{x}_{1\perp}} U^\dagger_{\vec{x}_{2\perp}} \right]$$

- Here U is the adjoint Wilson line on a light cone,

$$U_{\vec{x}_\perp} = \mathrm{P} \exp \left\{ i \, g \int\limits_{-\infty}^{\infty} dx^- \, \mathcal{A}^+(x^+ = 0, x^-, \vec{x}_\perp) \right\}$$

JIMWLK Equation

- JIMWLK equation can be used to construct any-N_C small-x evolution of any operator made of infinite light-cone Wilson lines (in any representation), such as color-dipole, color-quadrupole, etc., and other operators.

- Since
$$\Box\alpha(x^-, \vec{x}) \, = \, \rho(x^-, \vec{x})$$
JIMWLK evolution can be re-written in terms of the color density ρ in the kernel.

- JIMWLK approach sums up powers of $\alpha_s \, Y$ and $\alpha_s^2 \, A^{1/3}$

Solving JIMWLK

- The JIMWLK equation was solved on the lattice by K. Rummukainen and H. Weigert '04 (and others since).

- For the dipole amplitude $N(x_0,x_1, Y)$, the **relative** corrections to the large-N_C limit BK equation are **< 0.001 !** Not the naïve $1/N_C^2 \sim 0.1$! (For realistic rapidities/energies.)

- The reason for that is dynamical and is largely due to saturation effects suppressing the bulk of the potential $1/N_C^2$ corrections (Yu.K., J. Kuokkanen, K. Rummukainen, H. Weigert, '08).

Solution of the nonlinear equation

Solution of BK equation

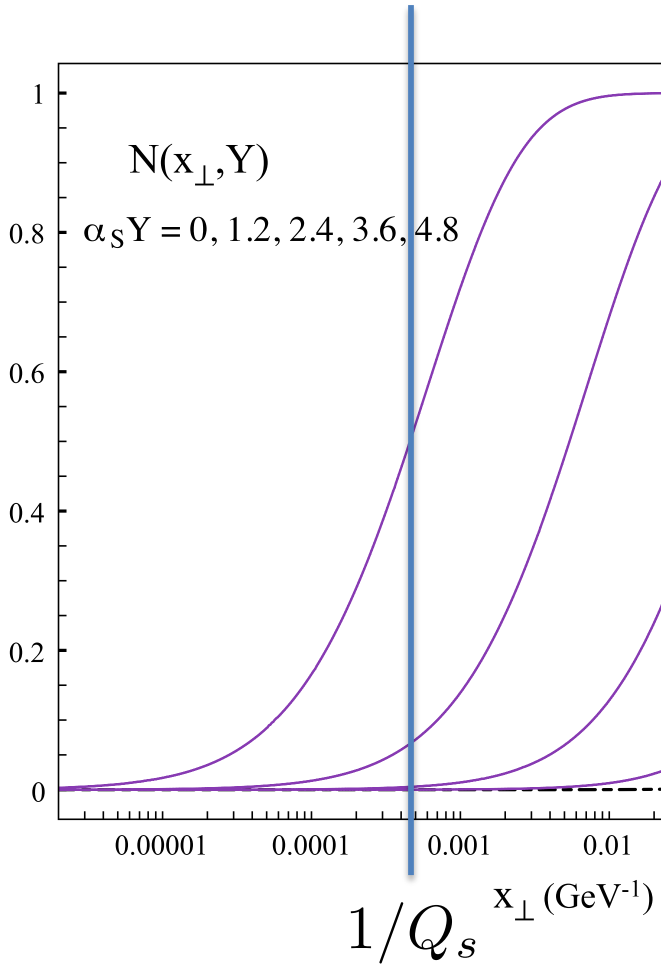

numerical solution
by J. Albacete '03
(earlier solutions were
found numerically by
Golec-Biernat, Motyka, Stasto,
by Braun, and by Lublinsky et al
in '01)

BK solution preserves the black disk limit, N<1 always
(unlike the linear BFKL equation)

$$\sigma^{q\bar{q}A} = 2 \int d^2b \, N(x_\perp, b_\perp, Y)$$

Saturation scale

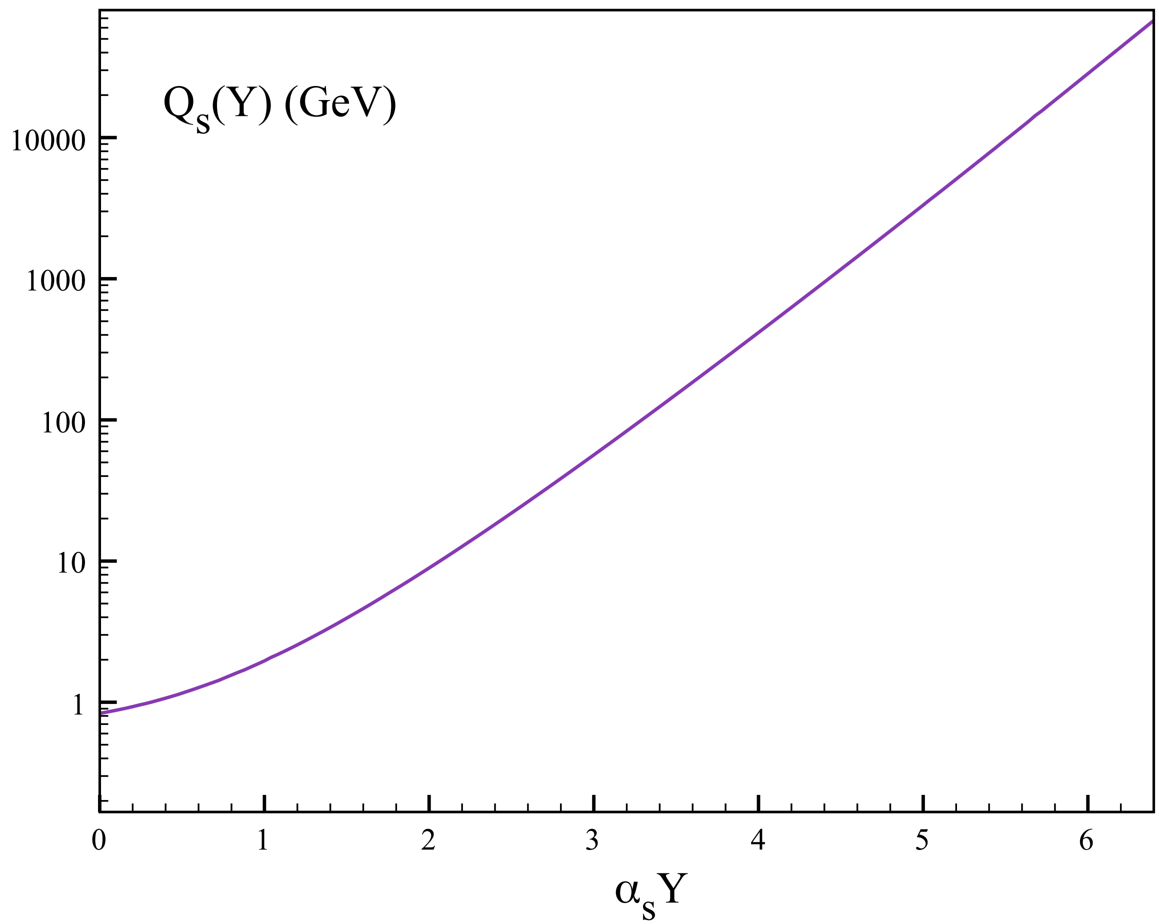

numerical solution by J. Albacete (ca. 2006)

BK Solution

- Preserves the black disk limit, N<1 always.

$$\sigma^{q\bar{q}A} = 2 \int d^2b\, N(x_\perp, b_\perp, Y)$$

- Avoids the IR problem of BFKL evolution due to the saturation scale screening the IR:

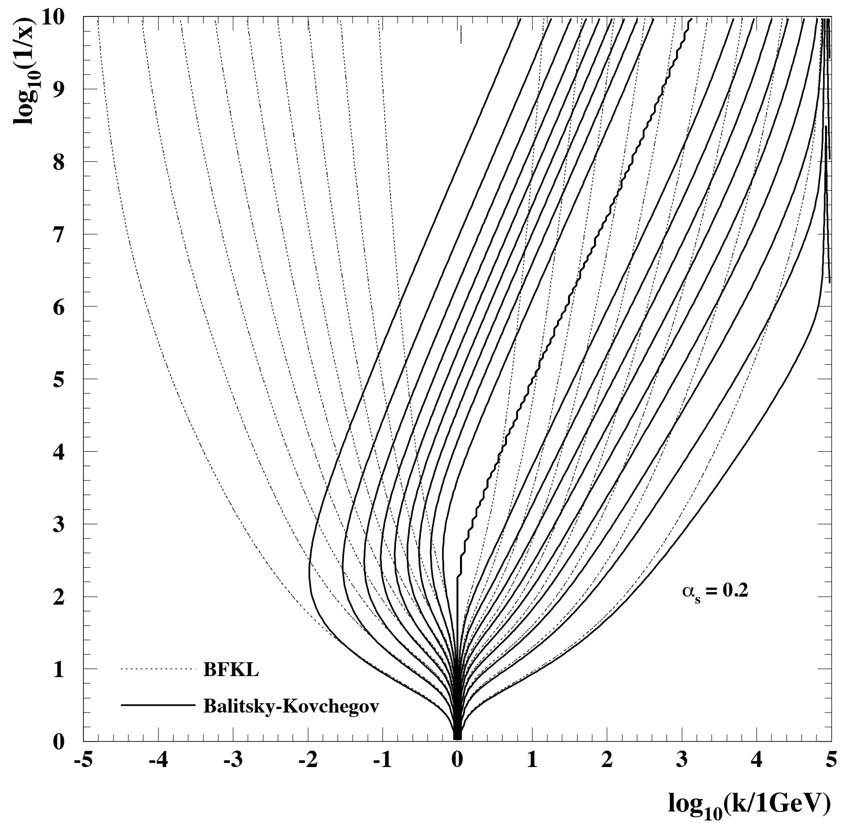

Golec-Biernat, Motyka, Stasto '02

The BFKL Equation




- The Balitsky, Fadin, Kuraev, Lipatov (BFKL) equation was derived in 1977-78.
- One starts with a two-gluon exchange diagram (left) and "dresses" it by radiative corrections.
- The leading high-energy contribution can be drawn as a ladder diagram, with the t-channel gluons being the special "reggeized" gluons and the thick dots representing effective Lipatov vertices.

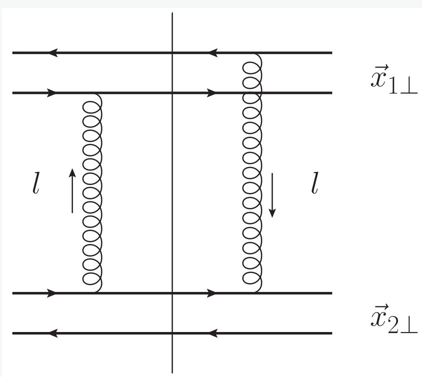

$$\frac{\partial f}{\partial \ln s} = \alpha_s \, K_{BFKL} \otimes f$$

The BFKL equation.
K_{BFKL} is an integral kernel.

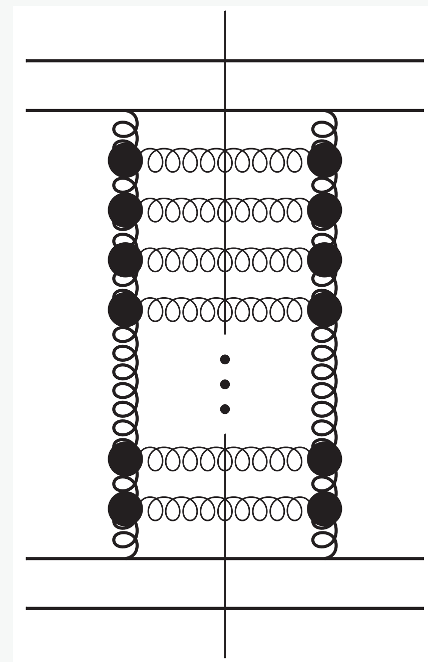

BFKL Equation

In the conventional Feynman diagram picture the BFKL equation can be represented by a ladder graph shown here. Each rung of the ladder brings in a power of α ln s.

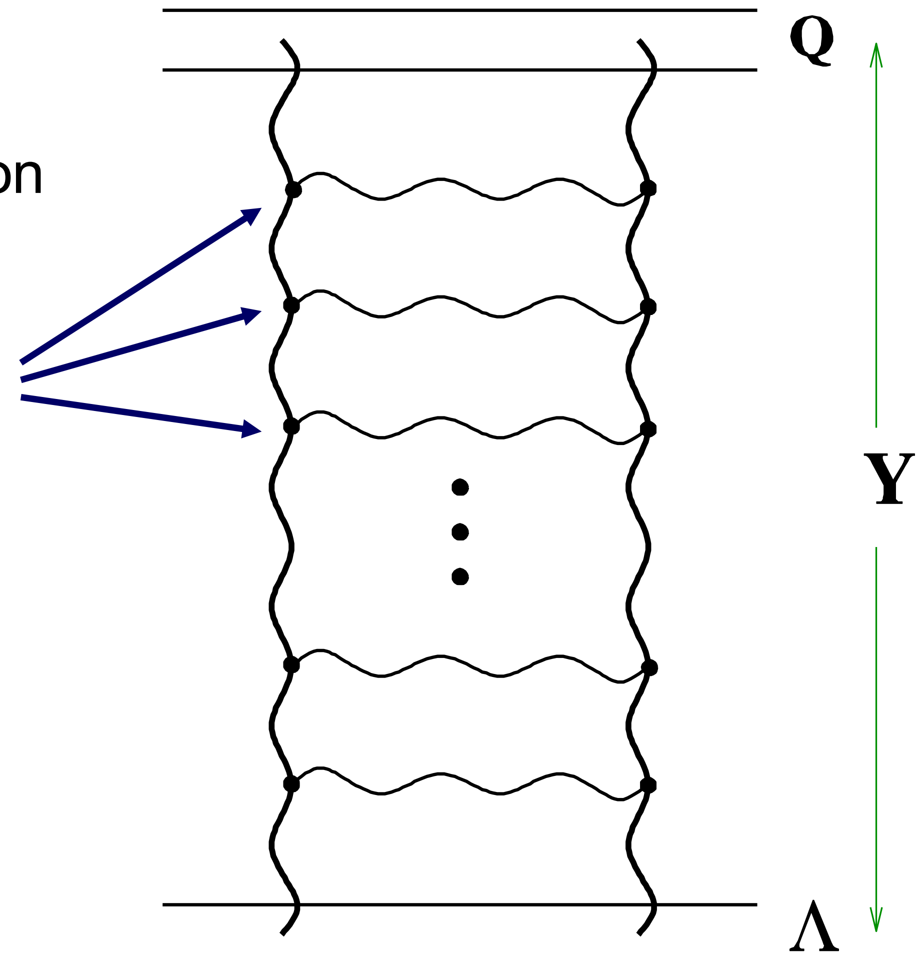

The resulting dipole amplitude grows as a power of energy

$$N \sim s^{\Delta}$$

violating Froissart unitarity bound

$$\sigma_{tot} \leq const \ln^2 s$$

GLR-MQ Equation

Gribov, Levin and Ryskin ('81)
proposed summing up "fan" diagrams:

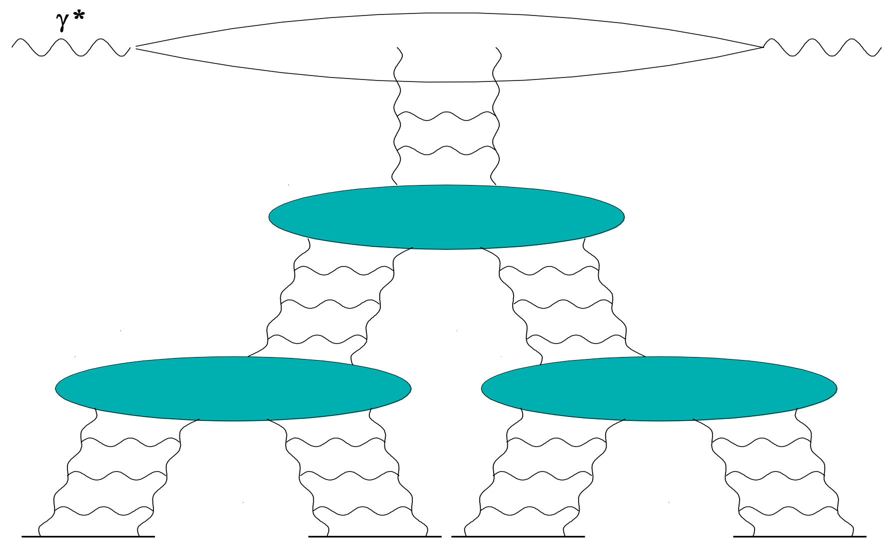

Mueller and Qiu (' 85) summed
"fan" diagrams for large Q^2.

The GLR-MQ equation reads:

$$\frac{\partial}{\partial \ln 1/x} \phi(x, k_T^2) = \alpha_s \, K_{BFKL} \otimes \phi(x, k_T^2) - \alpha_s \, [\phi(x, k_T^2)]^2$$

GLR-MQ equation has the same principle of recombination as BK and JIMWLK. GLR-MQ equation was thought about as the first nonlinear correction to the linear BFKL evolution. An AGL (Ayala, Gay Ducati, Levin '96) equation was suggested to resum higher-order nonlinear corrections.

BK/JIMWLK derivation showed that for the dipole amplitude N (!) there are no more terms in the large-N_C limit and obtained the correct kernel for the non-linear term (compared to GLR suggestion).

Energy Dependence of the Saturation Scale

Single BFKL ladder gives scattering amplitude of the order

$$N \sim \frac{\Lambda}{k_T}\, s^{\Delta}$$

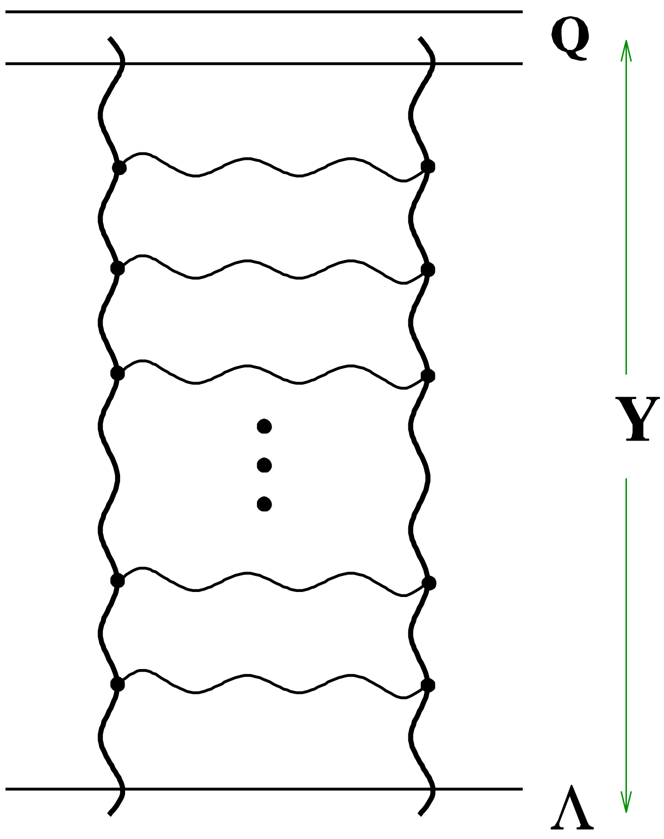

Nonlinear saturation effects become important when N ~ N^2 ⇨ N ~ 1. This happens at

$$\boxed{k_T = Q_s \sim \Lambda\, s^{\Delta}}$$

Saturation scale grows with energy!

Typical partons in the wave function have $k_T \sim Q_S$, so that their characteristic size is of the order $r \sim 1/k_T \sim 1/Q_S$.

⇨ Typical parton size decreases with energy!

Saturation scale

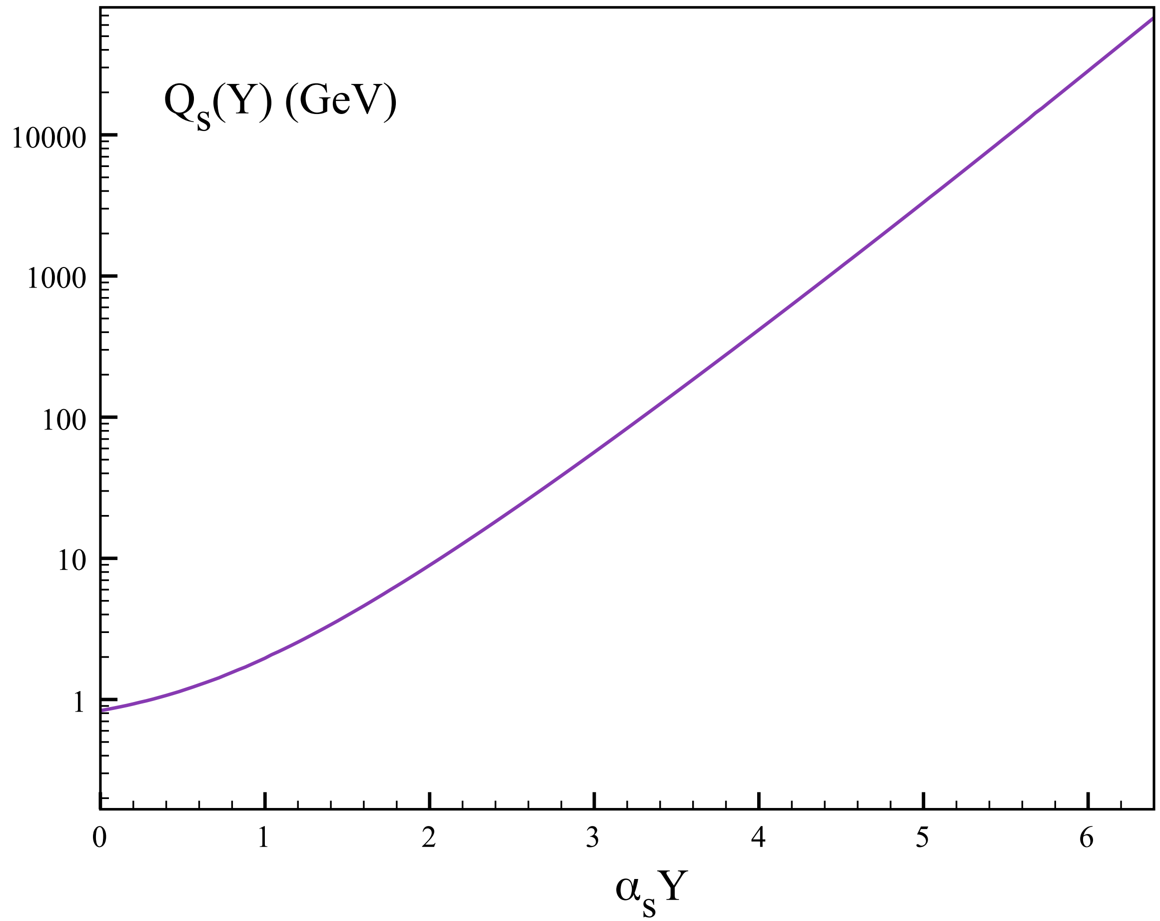

numerical solution by J. Albacete

High Density of Gluons

- High number of gluons populates the transverse extent of the proton or nucleus, leading to a very dense saturated wave function known as the Color Glass Condensate (CGC):

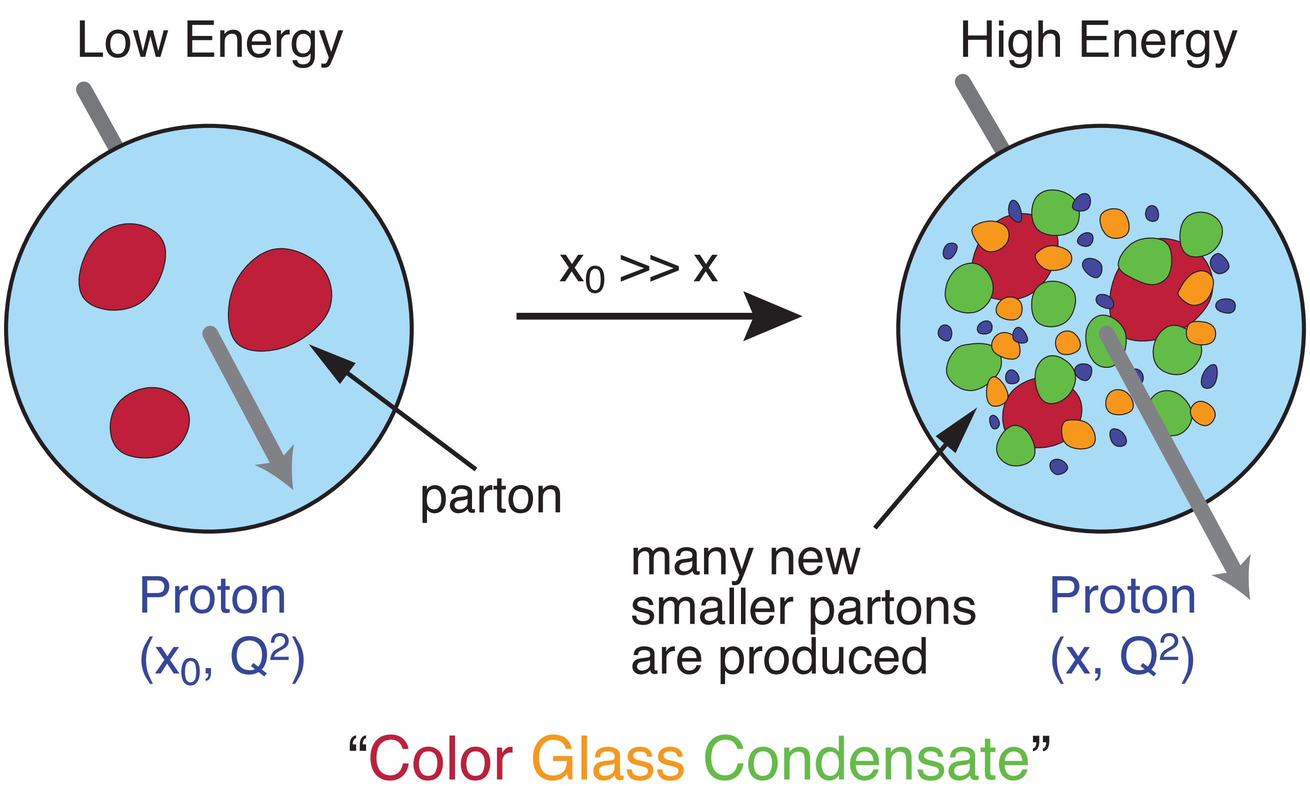

Map of High Energy QCD

energy

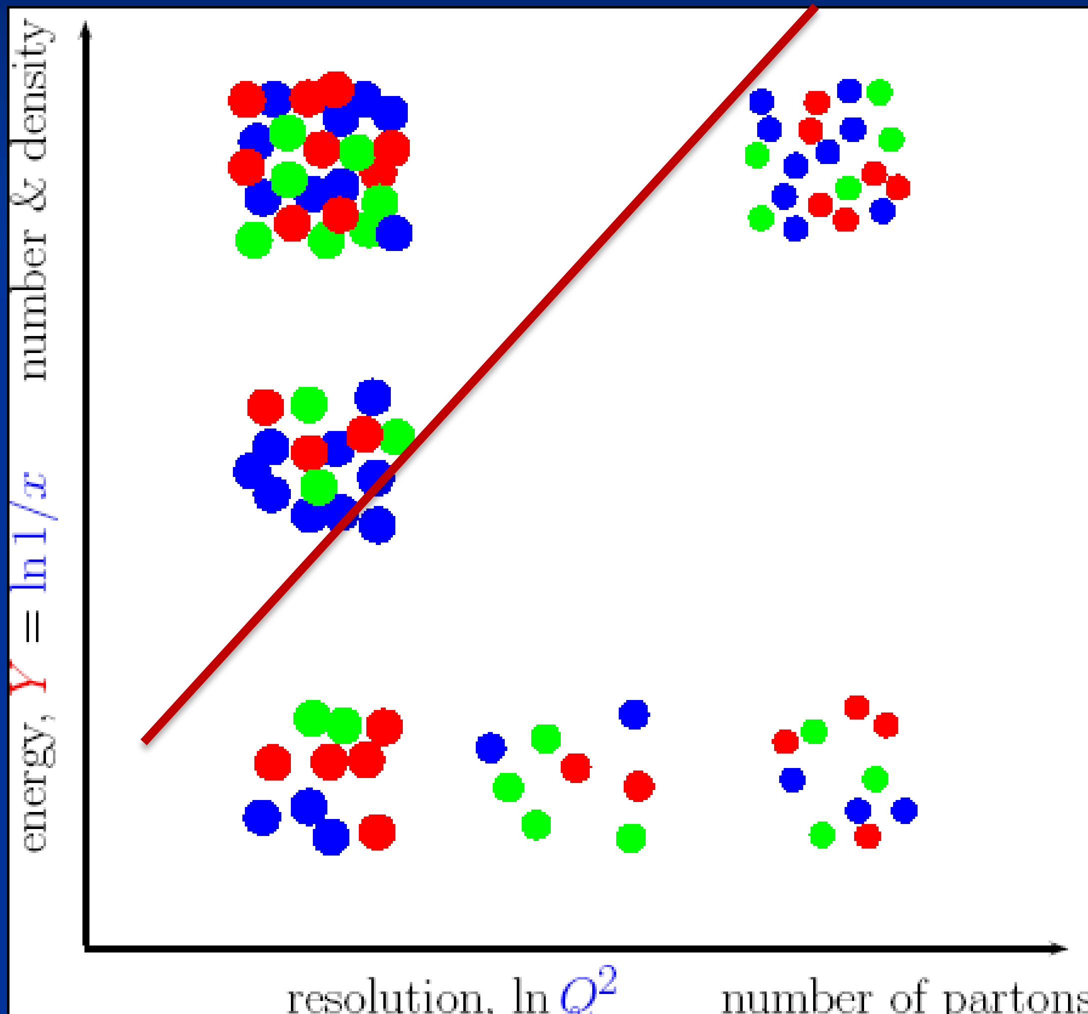

size of gluons

Map of High Energy QCD

energy

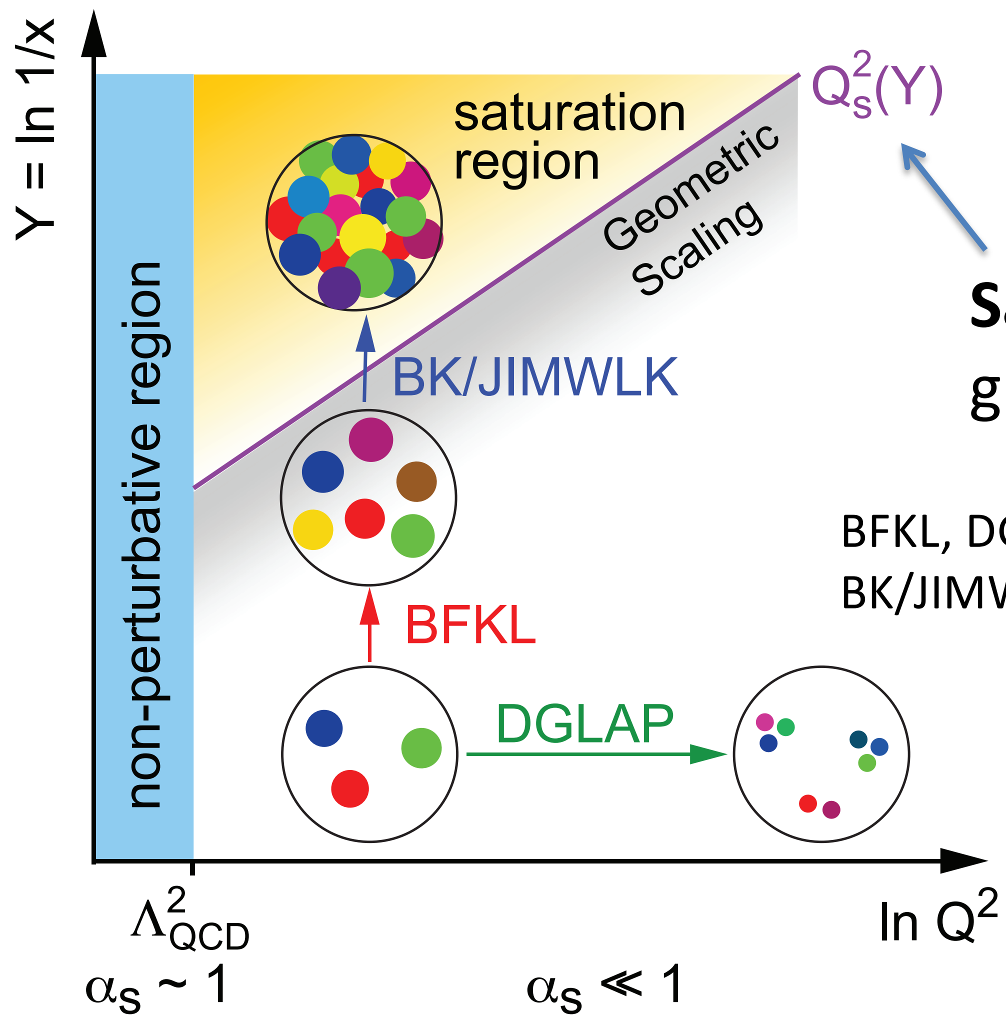

$$Q_s^2 \sim \left(\frac{1}{x}\right)^{\lambda}$$

Saturation Scale
grows with energy

BFKL, DGLAP – linear equations
BK/JIMWLK – nonlinear

size of gluons

Map of High Energy QCD

Saturation physics allows us to study regions of high parton density in the small coupling regime, where calculations are still under control!

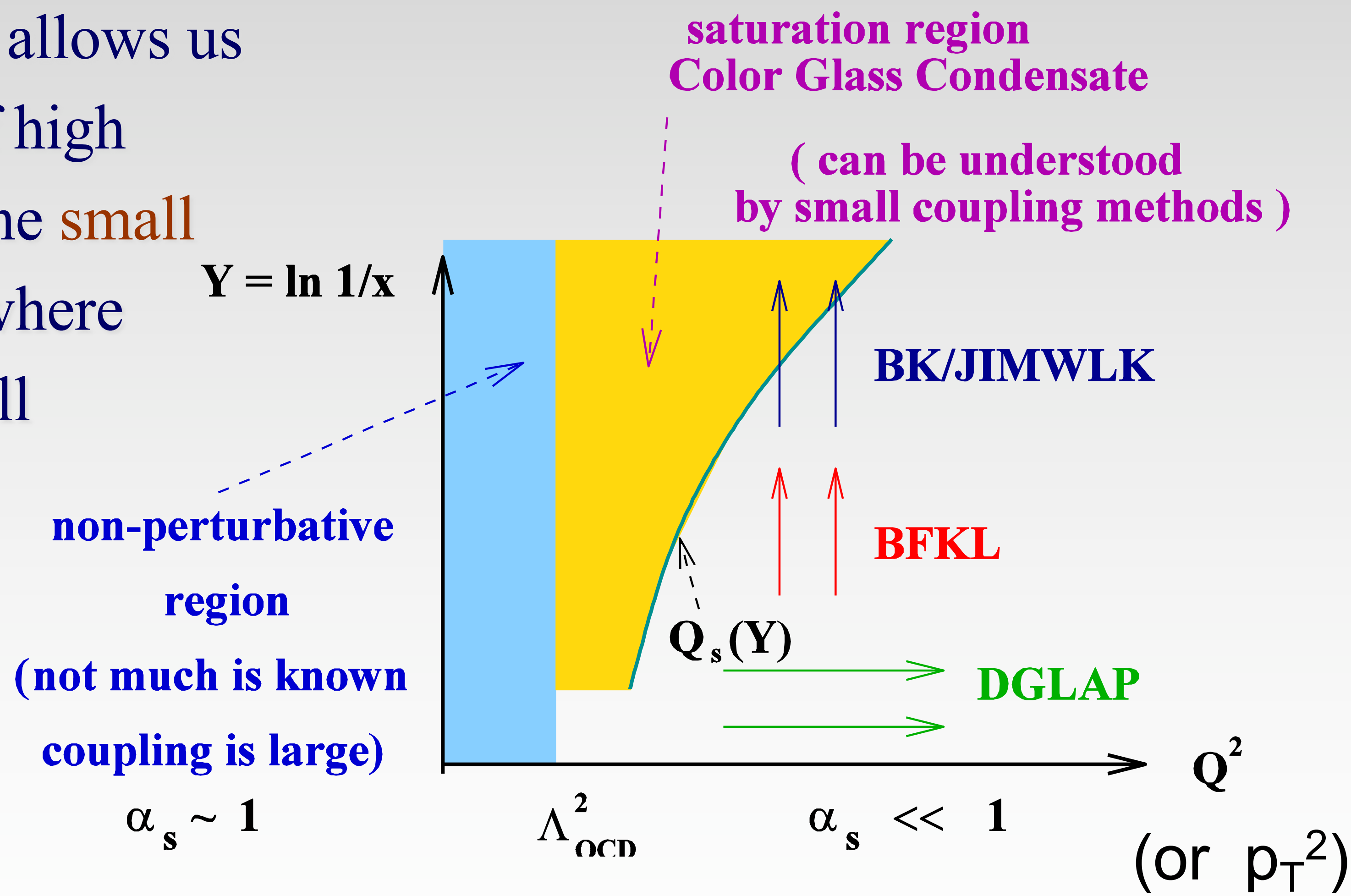

Transition to saturation region is characterized by the saturation scale

$$\boxed{Q_S^2 \sim A^{1/3}\left(\frac{1}{x}\right)^{\lambda}}$$

Saturation Scale

To summarize, saturation scale is an increasing function of both energy (1/x) and A:

$$Q_s^2 \sim \left(\frac{A}{x}\right)^{1/3}$$

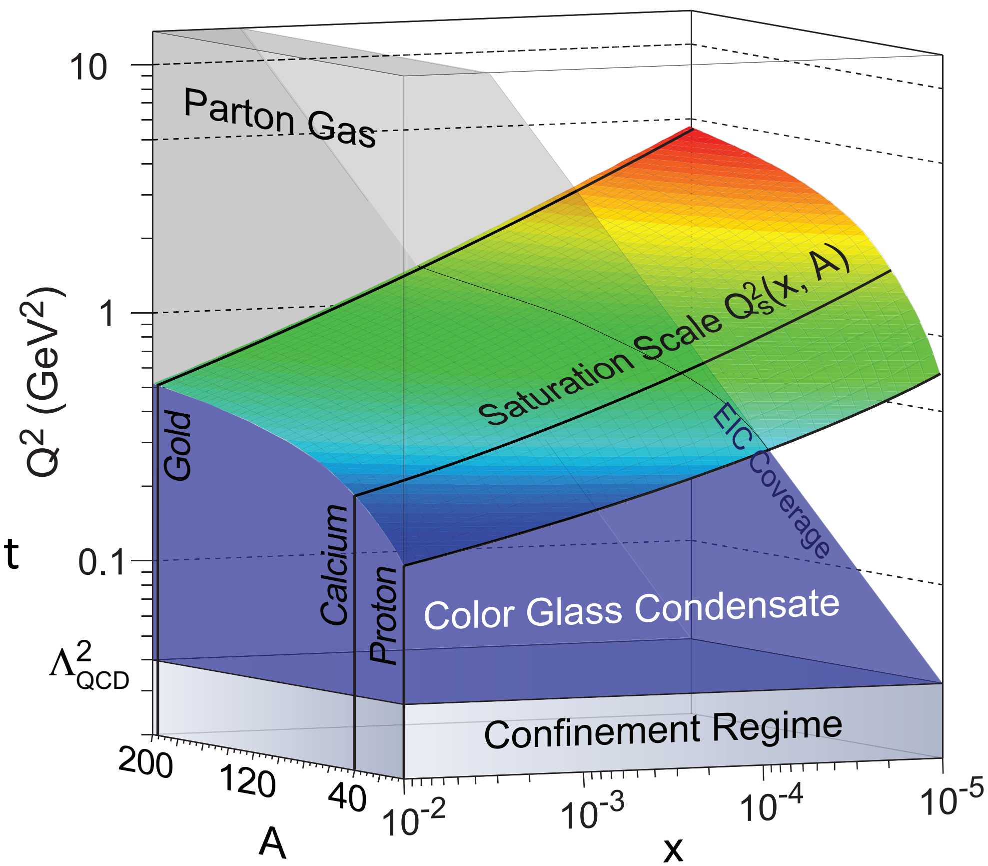

Gold nucleus provides an enhancement by $197^{1/3}$, which is equivalent to doing scattering on a proton at 197 times smaller x / higher s!

If you want to know more…

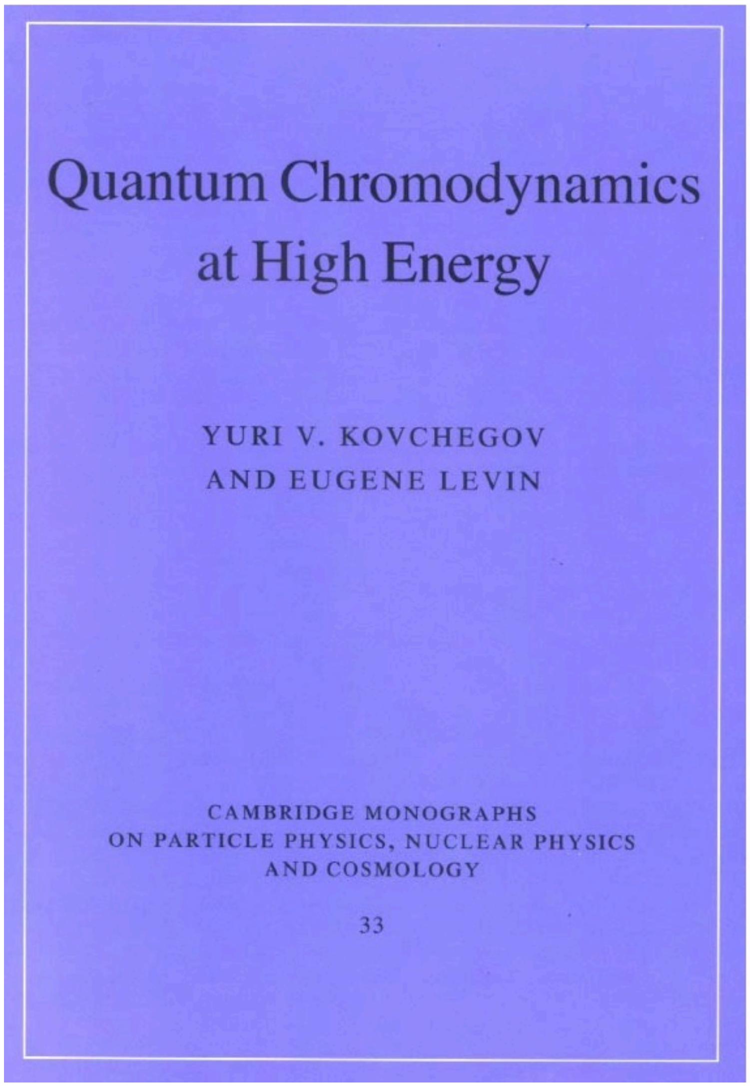

Published in September 2012
by Cambridge U Press

Saturation Physics at EIC

Electron-Ion Collider

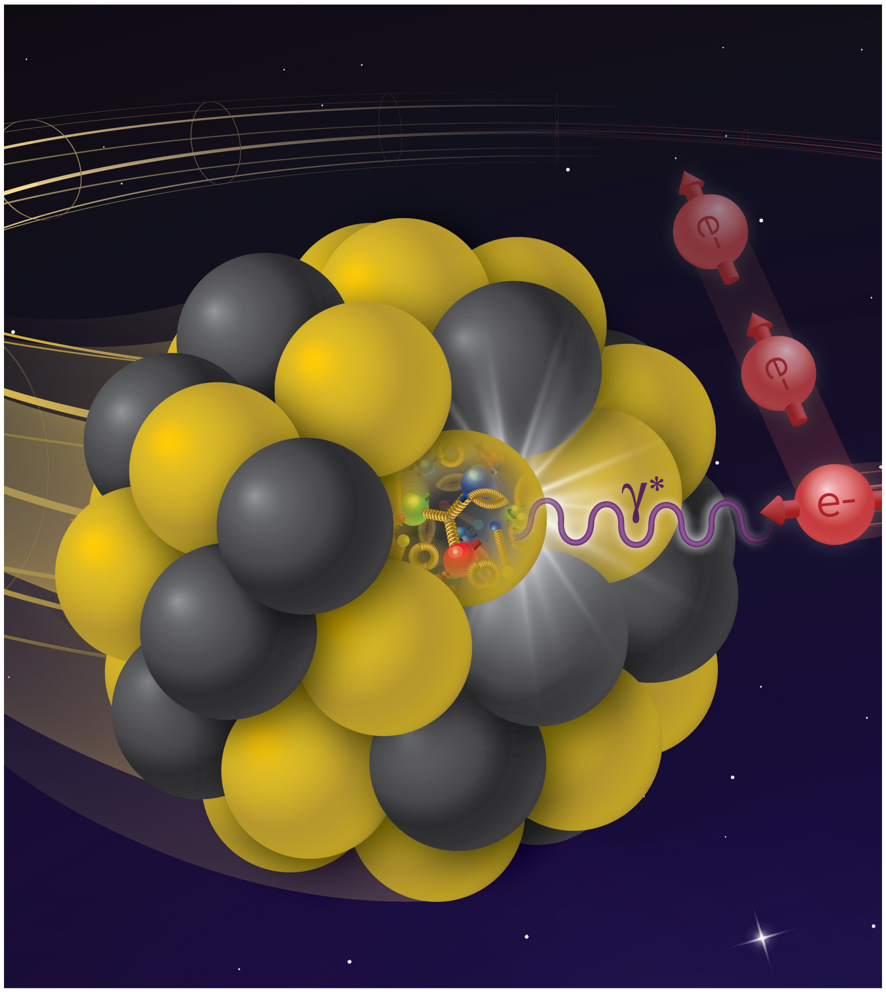

- Initial discussions about the EIC started back in the mid- to late-1990s.
- There was a number of workshops in the late 1990s and in 2000s dedicated to EIC physics.

Electron-Ion Collider (EIC) White Paper

- EIC WP was finished in late 2012 + 2nd edition in 2014
- A several-year effort by a 19-member steering committee + 58 co-authors
- arXiv:1212.1701 [nucl-ex]
- At the time EIC could be sited either at Brookhaven or at Jefferson Lab.

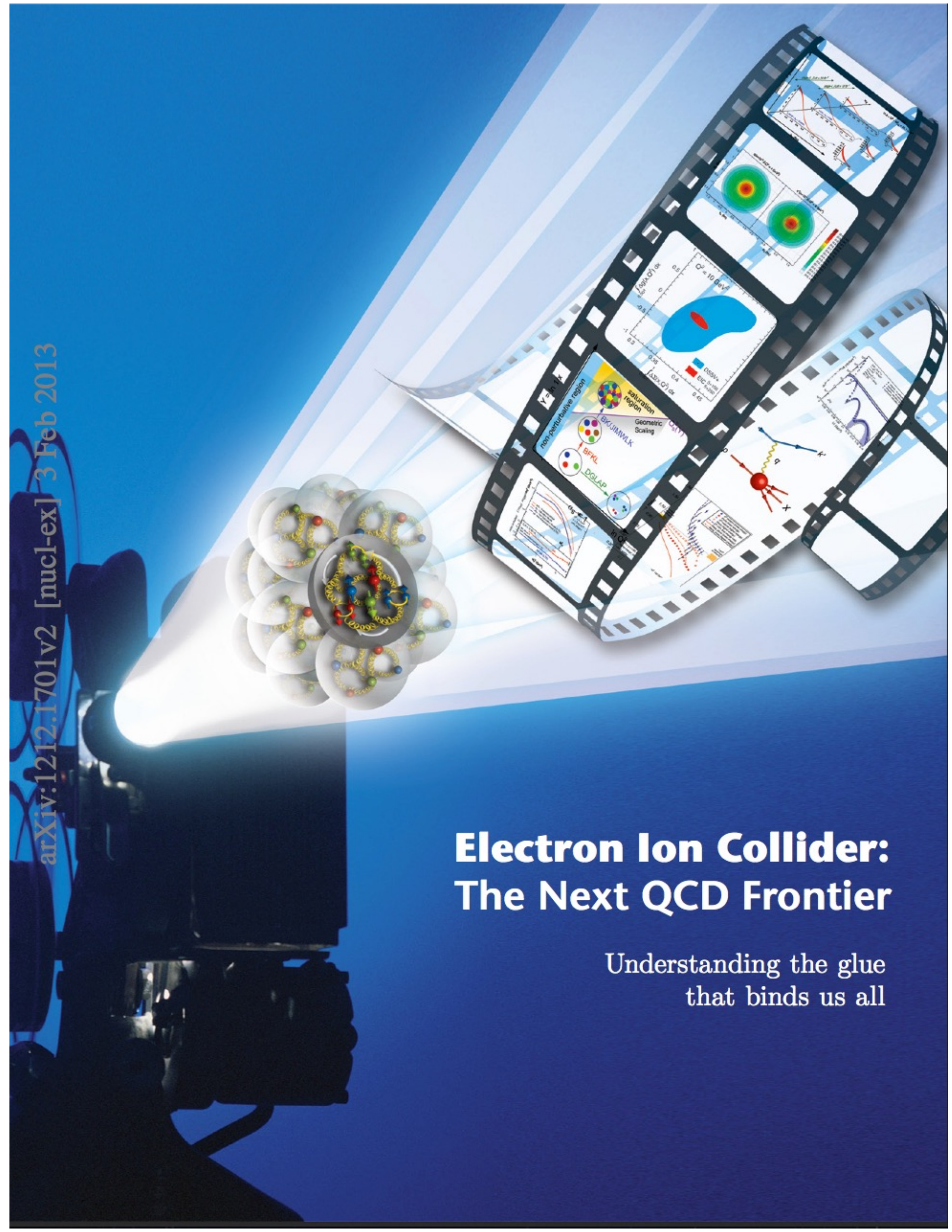

DOE Announcement on EIC

EIC is to be built at BNL

January 9, 2020

WASHINGTON, D.C. – Today, the **U.S. Department of Energy (DOE)** announced the selection of Brookhaven National Laboratory in Upton, NY, as the site for a planned major new nuclear physics research facility.

The Electron Ion Collider (EIC), to be designed and constructed over ten years at an estimated cost between $1.6 and $2.6 billion, will smash electrons into protons and heavier atomic nuclei in an effort to penetrate the mysteries of the "strong force" that binds the atomic nucleus together.

"The EIC promises to keep America in the forefront of nuclear physics research and particle accelerator technology, critical components of overall U.S. leadership in science," said **U.S. Secretary of Energy Dan Brouillette**. "This facility will deepen our understanding of nature and is expected to be the source of insights ultimately leading to new technology and innovation."

"America is in the golden age of innovation, and we are eager to take this next step with EIC. The EIC will not only ensure U.S. leadership in nuclear physics, but the technology developed for EIC will also support potential tremendous breakthroughs impacting human health, national competiveness, and national security," said **Under Secretary for Science Paul Dabbar**. "We look forward to our continued world-leading scientific discoveries in conjunction with our international partners."

The EIC's high luminosity and highly polarized beams will push the frontiers of particle accelerator science and technology and provide unprecedented insights into the building blocks and forces that hold atomic nuclei together.

Design and construction of an EIC was recommended by the National Research Council of the National Academies of Science, noting that such a facility "would maintain U.S. leadership in nuclear physics" and "help to maintain scientific leadership more broadly." Plans for an EIC were also endorsed by the federal Nuclear Science Advisory Committee.

Secretary Brouillette approved Critical Decision-0, "Approve Mission Need," for the EIC on December 19, 2019.

Can Saturation be Discovered at EIC?

EIC has an unprecedented small-x reach for DIS on large nuclear targets, allowing to seal the discovery of saturation physics and study of its properties:

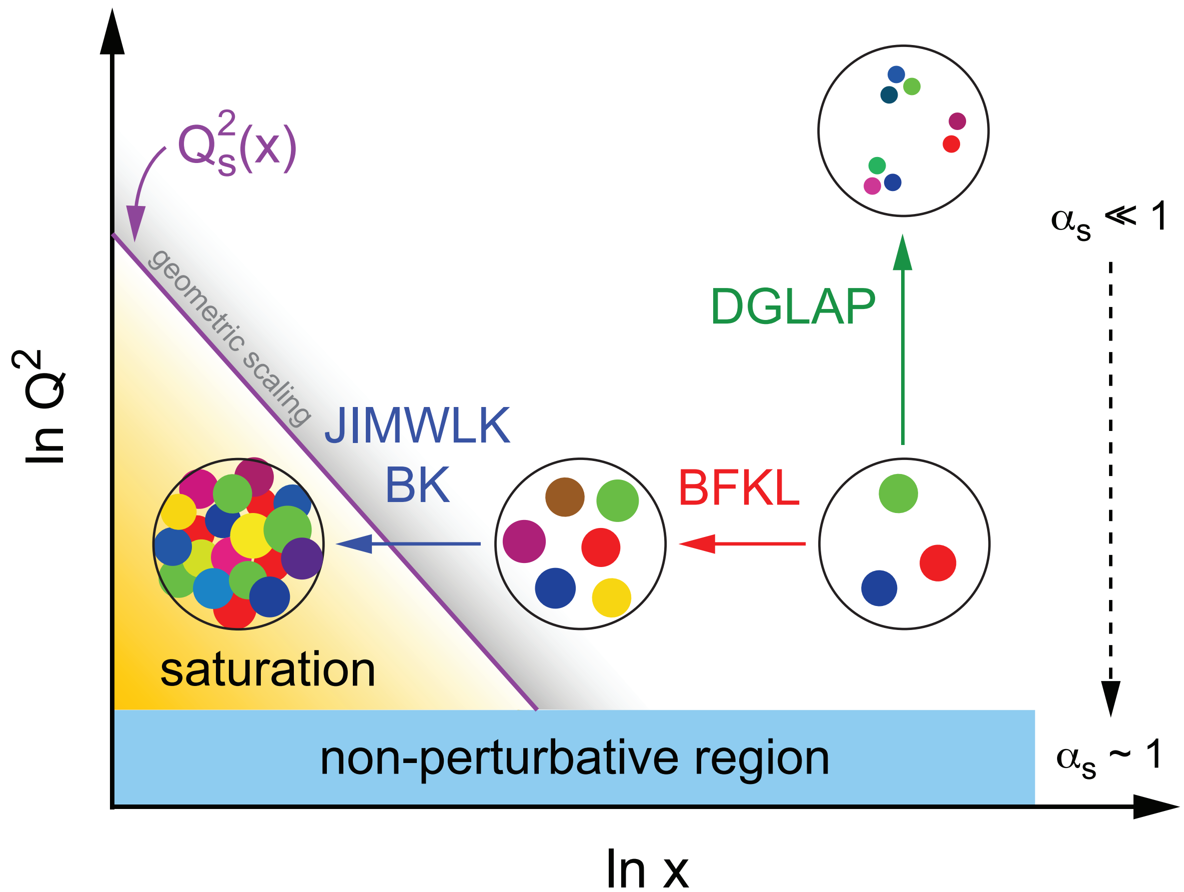

Can Saturation be Discovered at EIC?

EIC has an unprecedented small-x reach for DIS on large nuclear targets, allowing to seal the discovery of saturation physics and study of its properties:

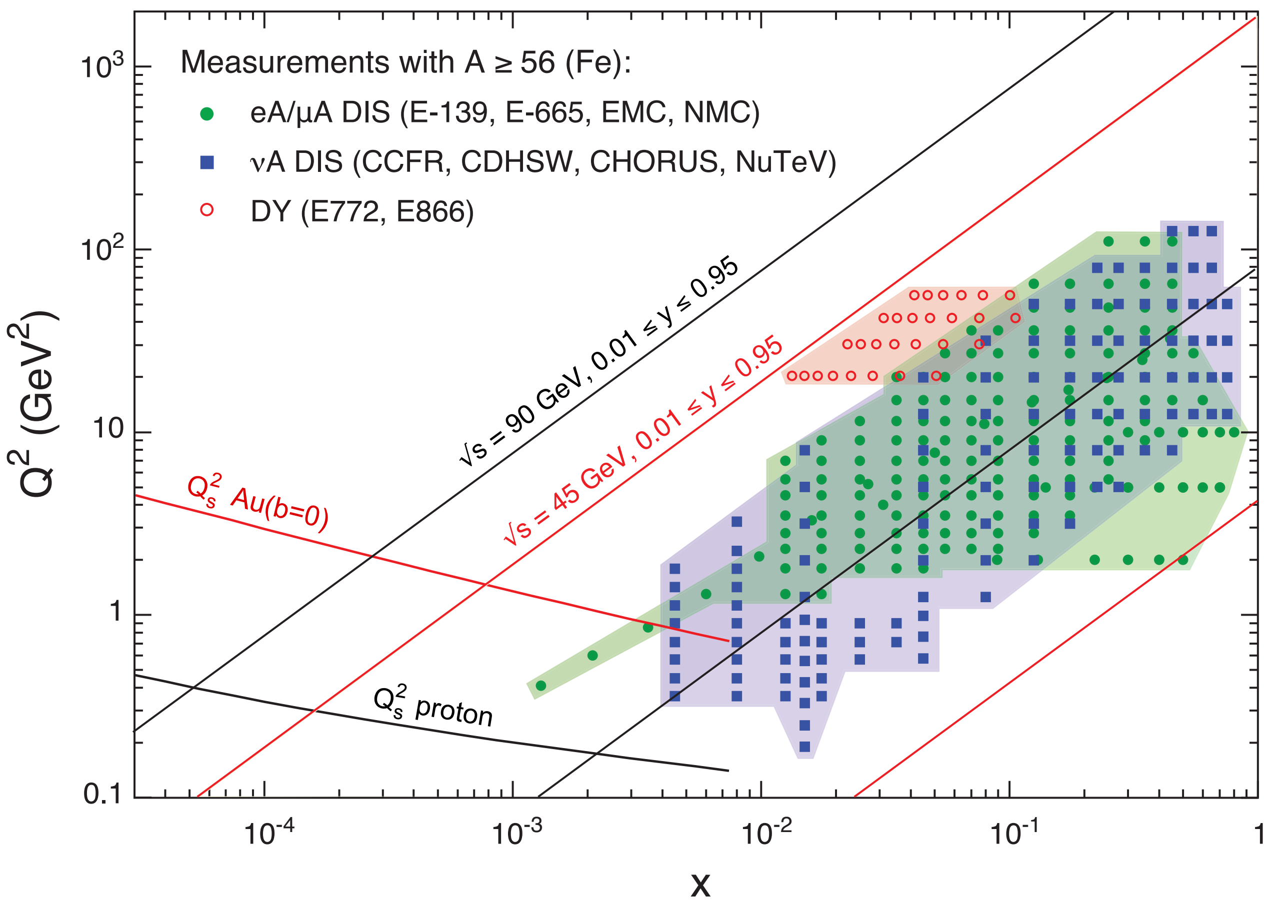

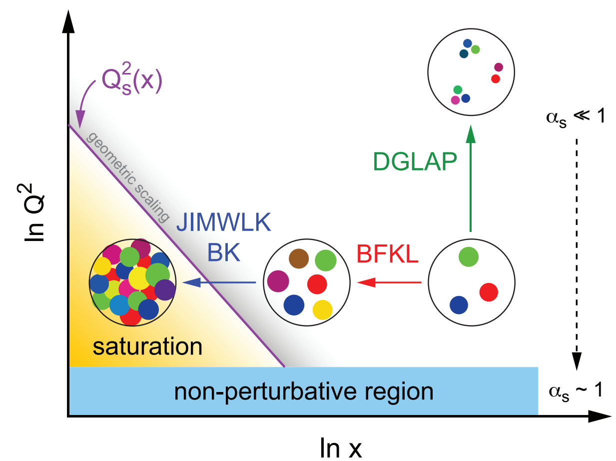

(i) Nuclear Structure Functions

Structure Functions at EIC

Nuclear structure functions F_2 and F_L (parts of σ^{e+A} cross section) which will be measured at EIC (values = EPS09+PYTHIA). Shaded area = (x, Q^2) range of the world e+A data.

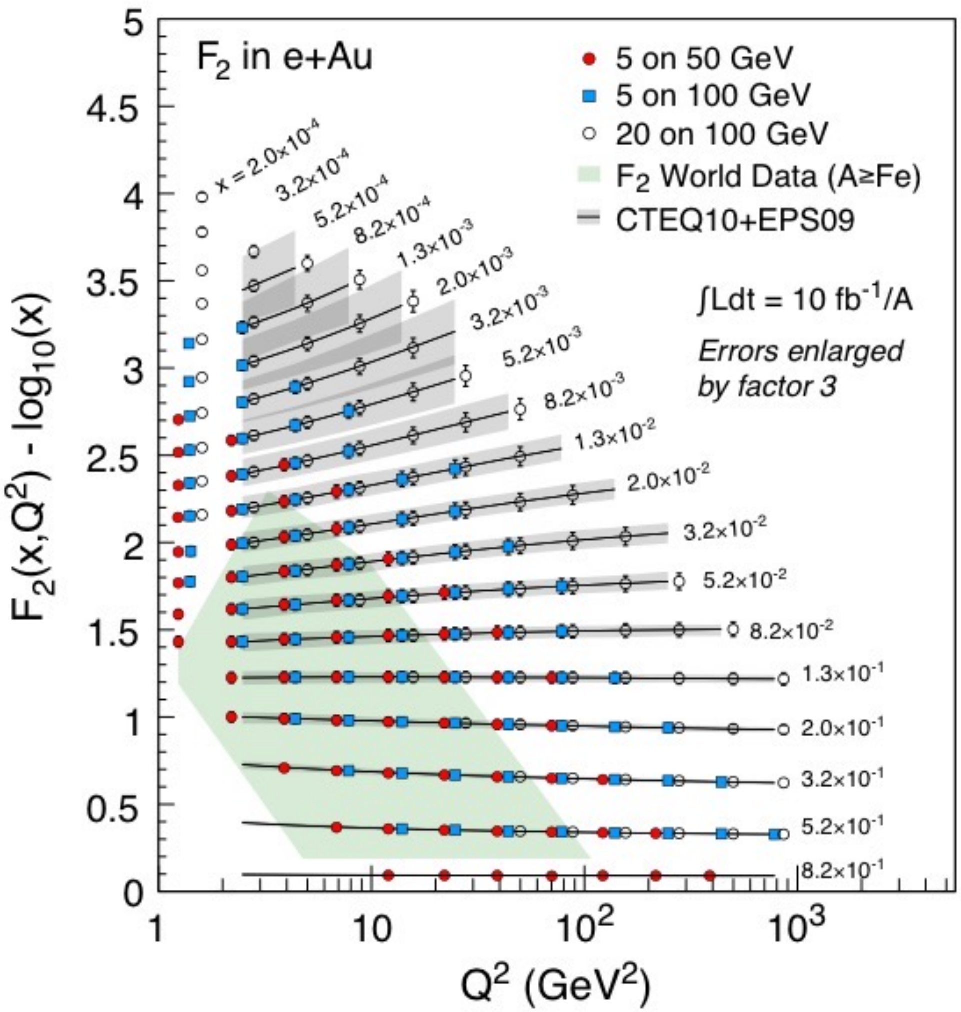

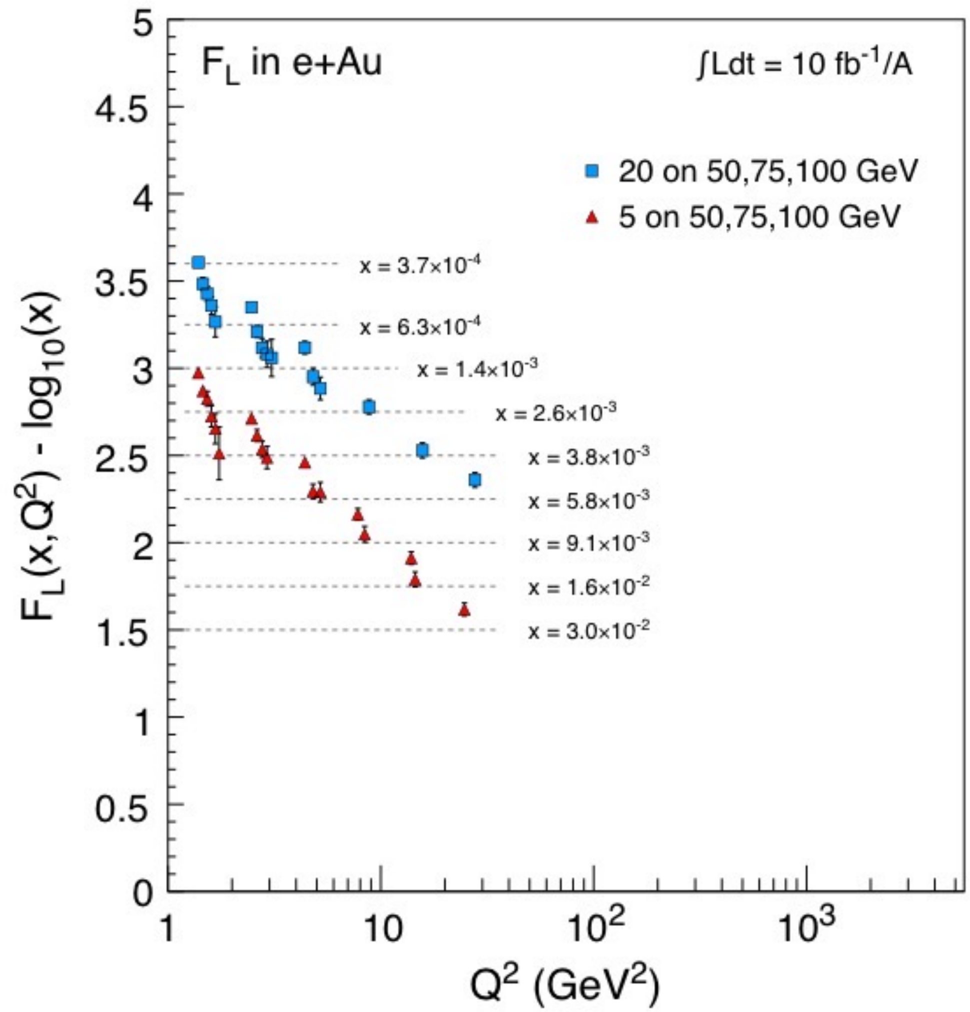

Nuclear Shadowing

- Saturation effects may explain nuclear shadowing: reduction of the number of gluons per nucleon with decreasing x and/or increasing A:

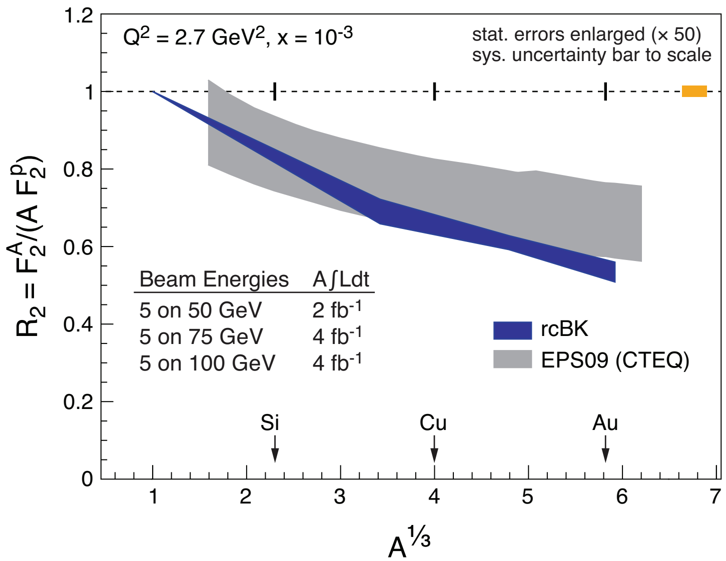

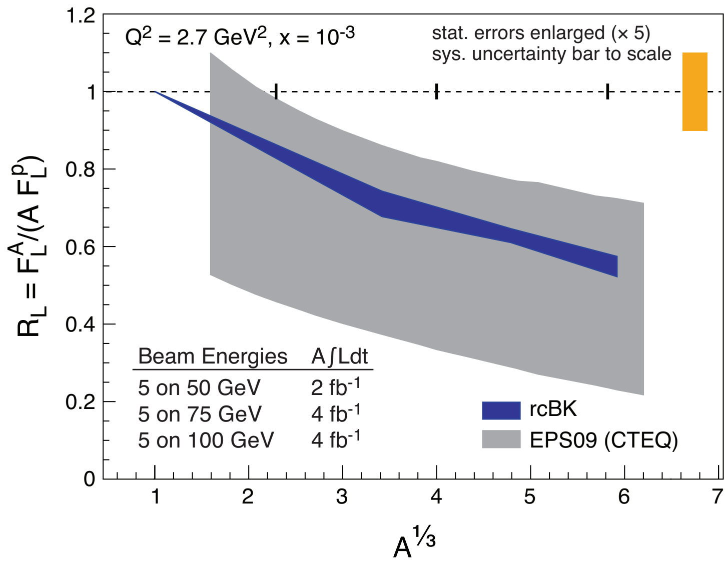

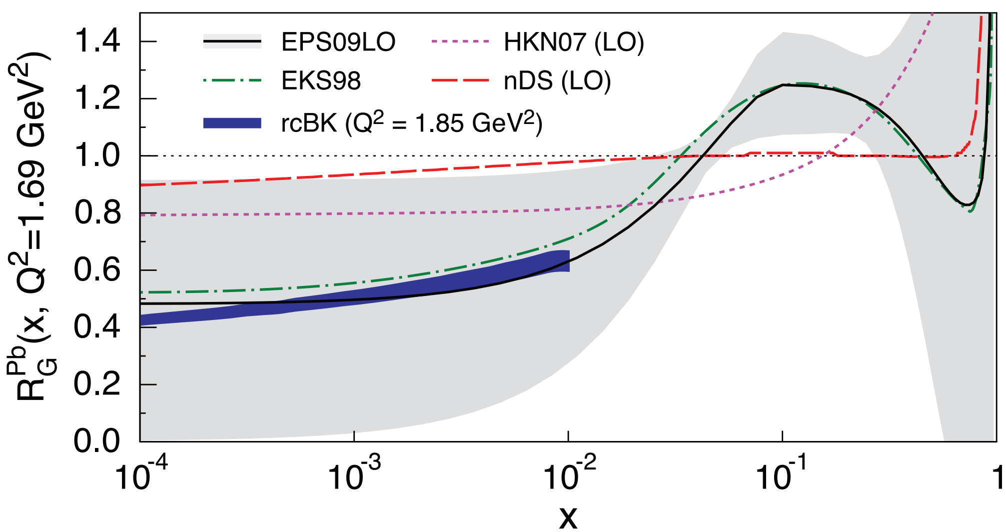

But: as DGLAP does not predict the x- and A-dependences, it needs to be constrained by the data.

Note that including heavy flavors (charm) for F_2 and F_L should help distinguish between the saturation versus non-saturation predictions.

Nuclear Shadowing for Charm

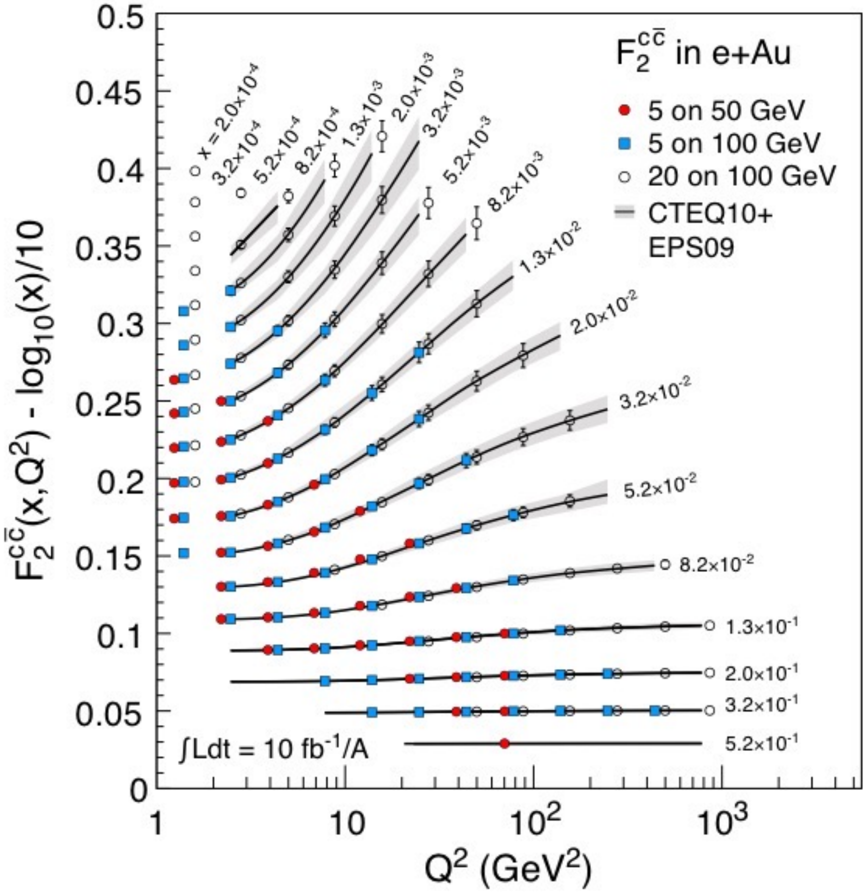

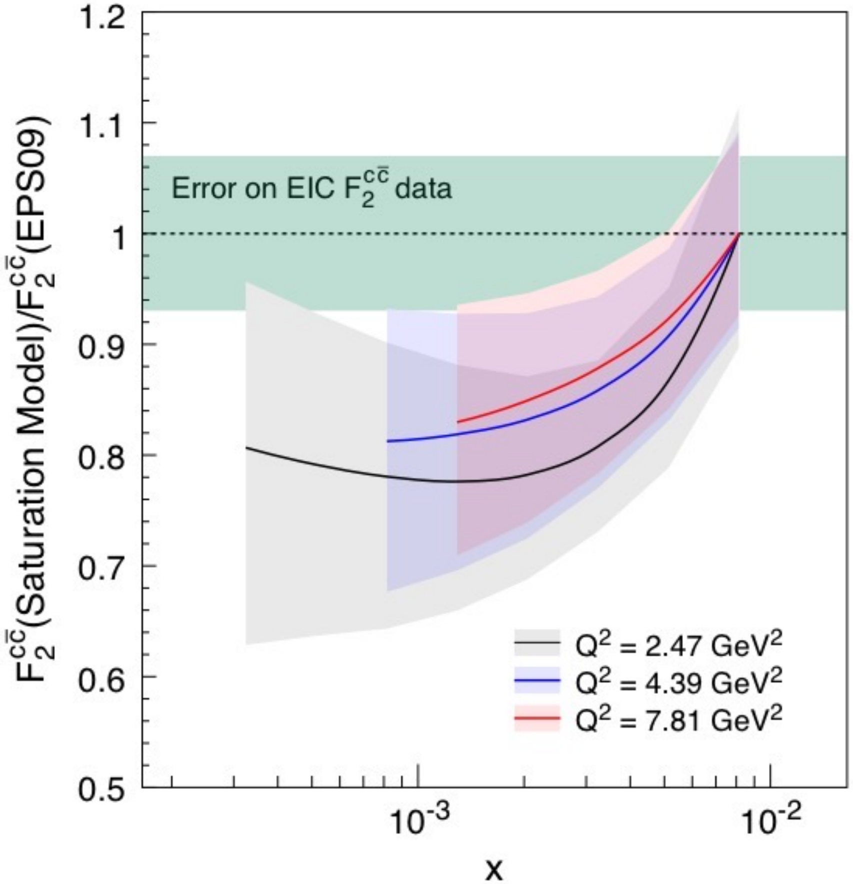

may help distinguish saturation vs DGLAP-based prediction

(ii) Di-Hadron Correlations

De-correlation

- Small-x evolution ↔ multiple emissions
- Multiple emissions → de-correlation.

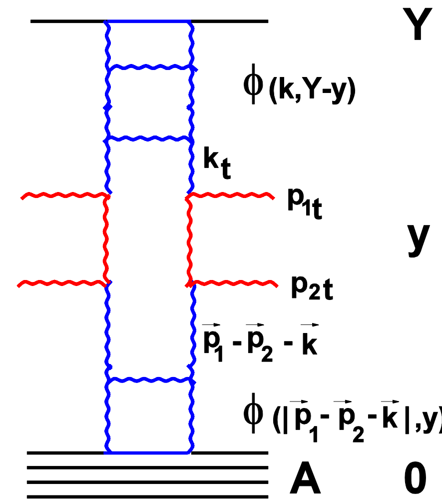

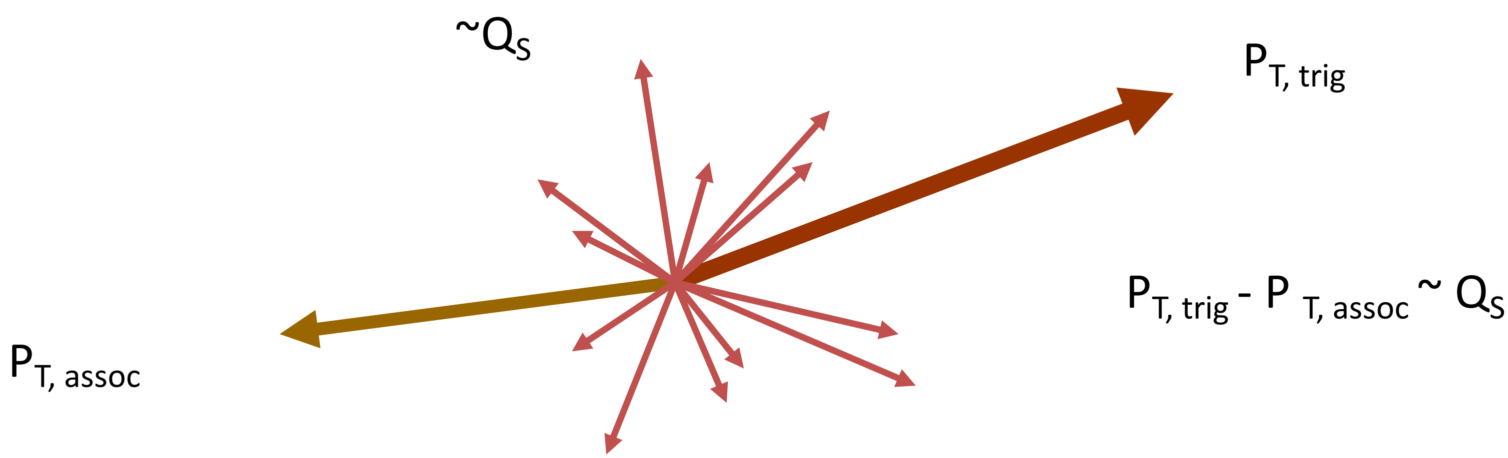

- B2B jets may get de-correlated in p_T with the spread of the order of Q_S

Di-hadron Correlations

Depletion of di-hadron correlations is predicted for e+A as compared to e+p. (Dominguez et al ‘11; Zheng et al ‘14). This is a signal of saturation.

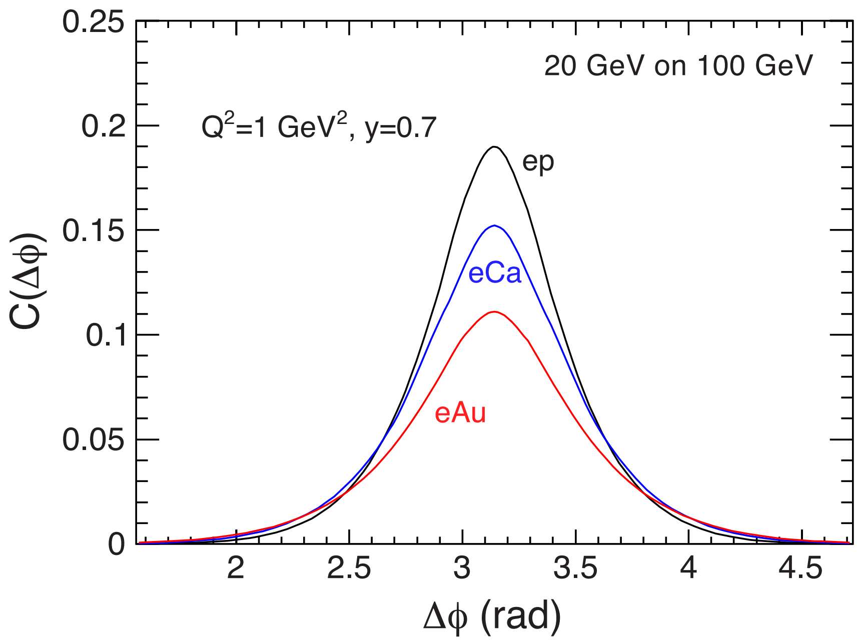

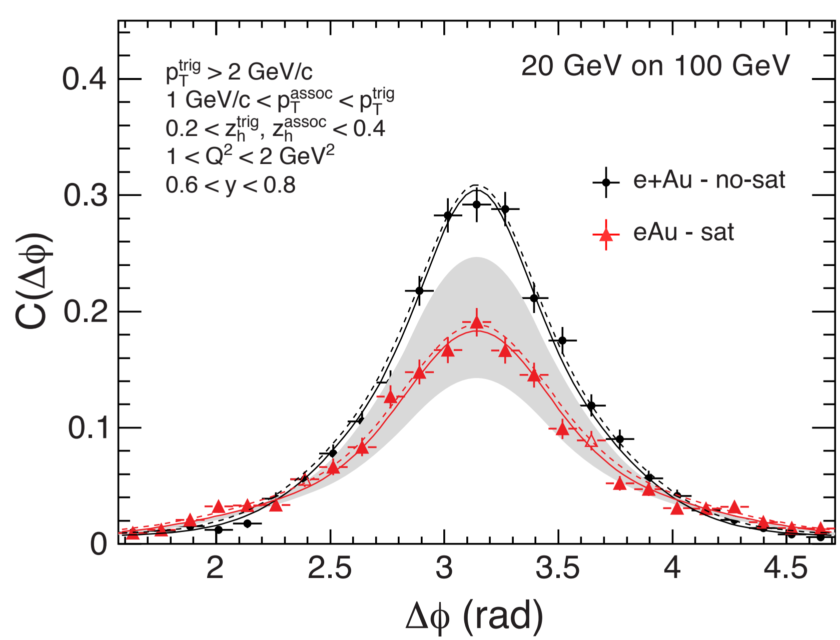

(iii) Diffraction

Diffraction terminology

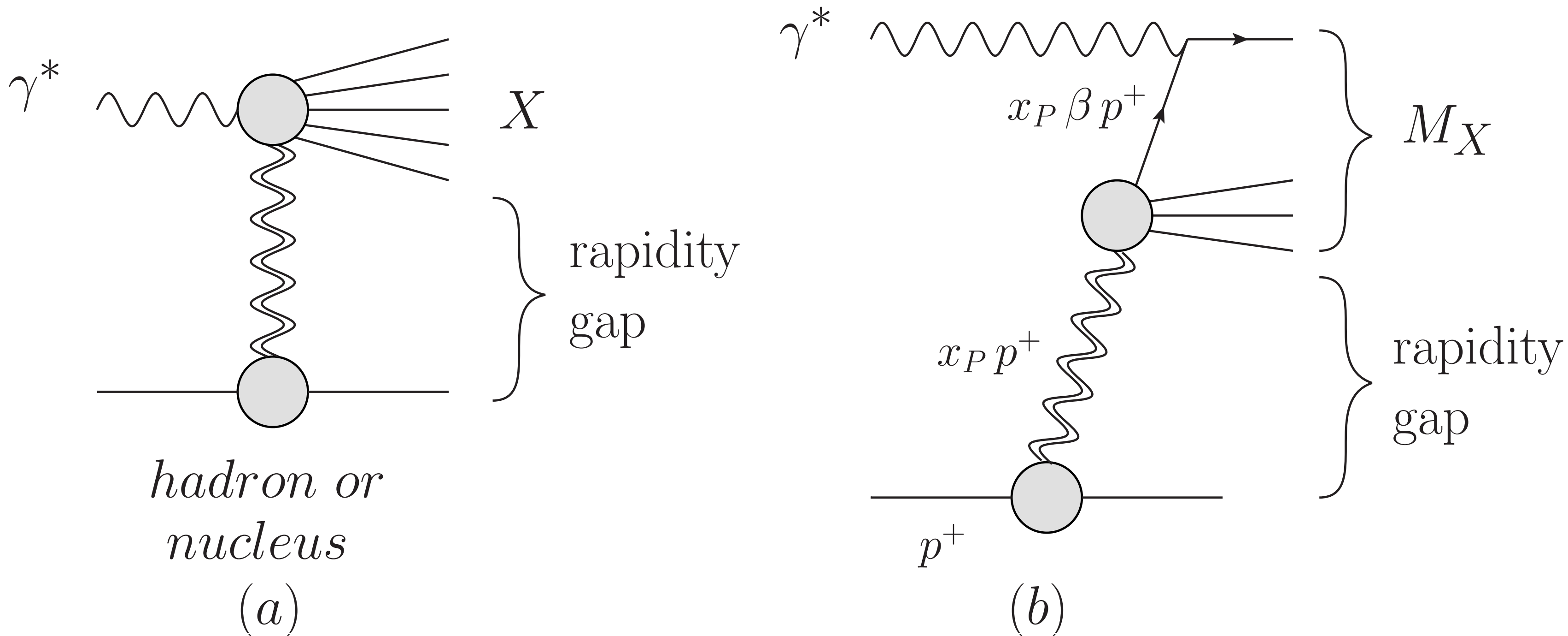

$$x_P = \frac{Q^2 + M_X^2}{Q^2 + W^2} \qquad \beta = \frac{x_{Bj}}{x_P} = \frac{Q^2}{Q^2 + M_X^2}$$

Quasi-elastic DIS

Consider the case when nothing but the quark-antiquark pair (pions) is produced:

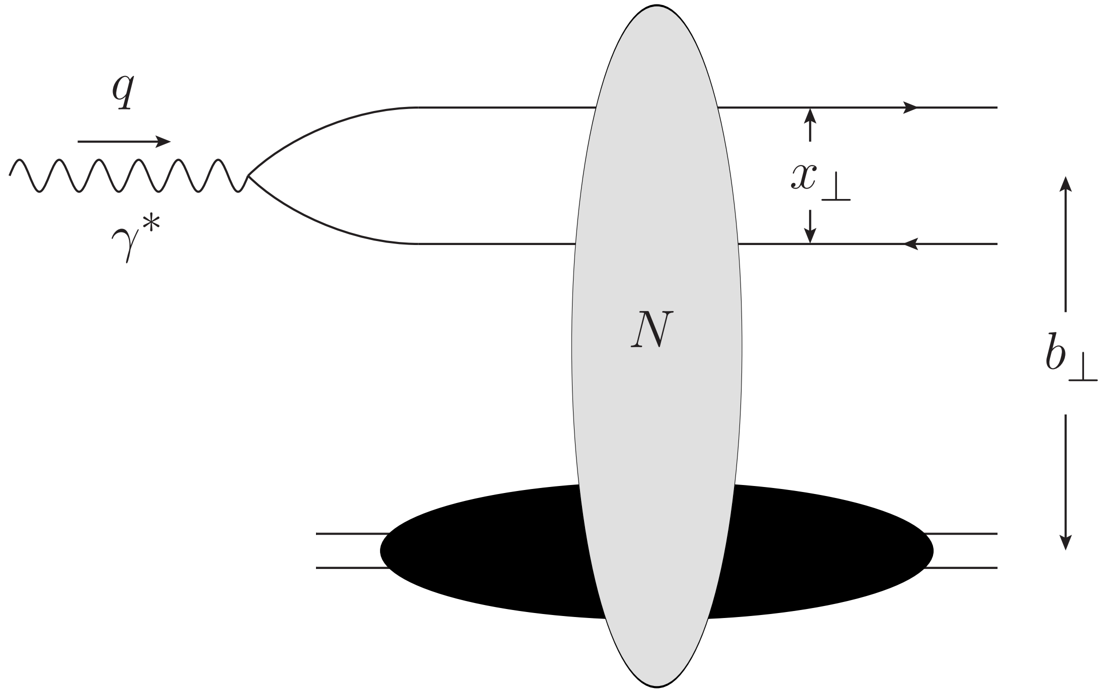

The quasi-elastic cross section is then

$$\sigma_{el}^{\gamma^* A} = \int \frac{d^2 x_\perp}{4\,\pi}\, d^2 b_\perp \int\limits_0^1 \frac{dz}{z\,(1-z)}\, |\Psi^{\gamma^* \to q\bar{q}}(\vec{x}_\perp, z)|^2 \, N^2(\vec{x}_\perp, \vec{b}_\perp, Y)$$

Buchmuller et al '97, McLerran and Yu.K. '99

Diffraction on a black disk

- For low Q^2 (large dipole sizes) the black disk limit is reached with N=1
- Diffraction (elastic scattering) becomes a half of the total cross section

$$\frac{\sigma_{el}^{q\bar{q}A}}{\sigma_{tot}^{q\bar{q}A}} = \frac{\int d^2b\, N^2}{2\ \int d^2b\, N} \longrightarrow \frac{1}{2}$$

- Large fraction of diffractive events in DIS is a signature of reaching the black disk limit!
- HERA: ~15% (unexpected!) ; EIC: ~25% expected from saturation

Diffractive over total cross sections

- Here's an early EIC measurement which may **distinguish saturation from non-saturation** approaches:

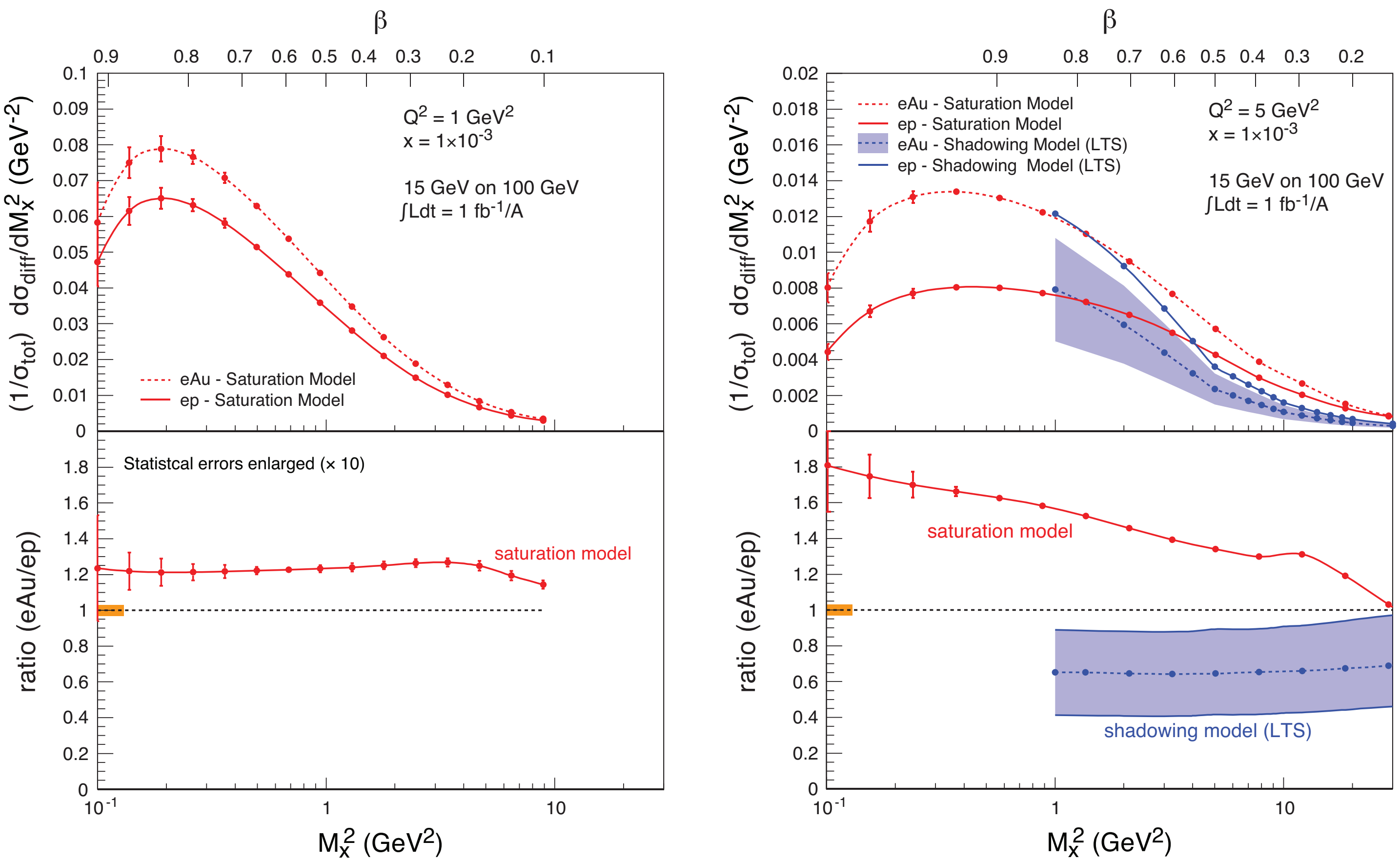

sat = Kowalski et al '08, plots generated by Marquet

no-sat = Leading Twist Shadowing (LTS), Frankfurt, Guzey, Strikman '04, plots by Guzey

Exclusive Vector Meson Production

- An important diffractive process which can be measured at EIC is exclusive vector meson production:

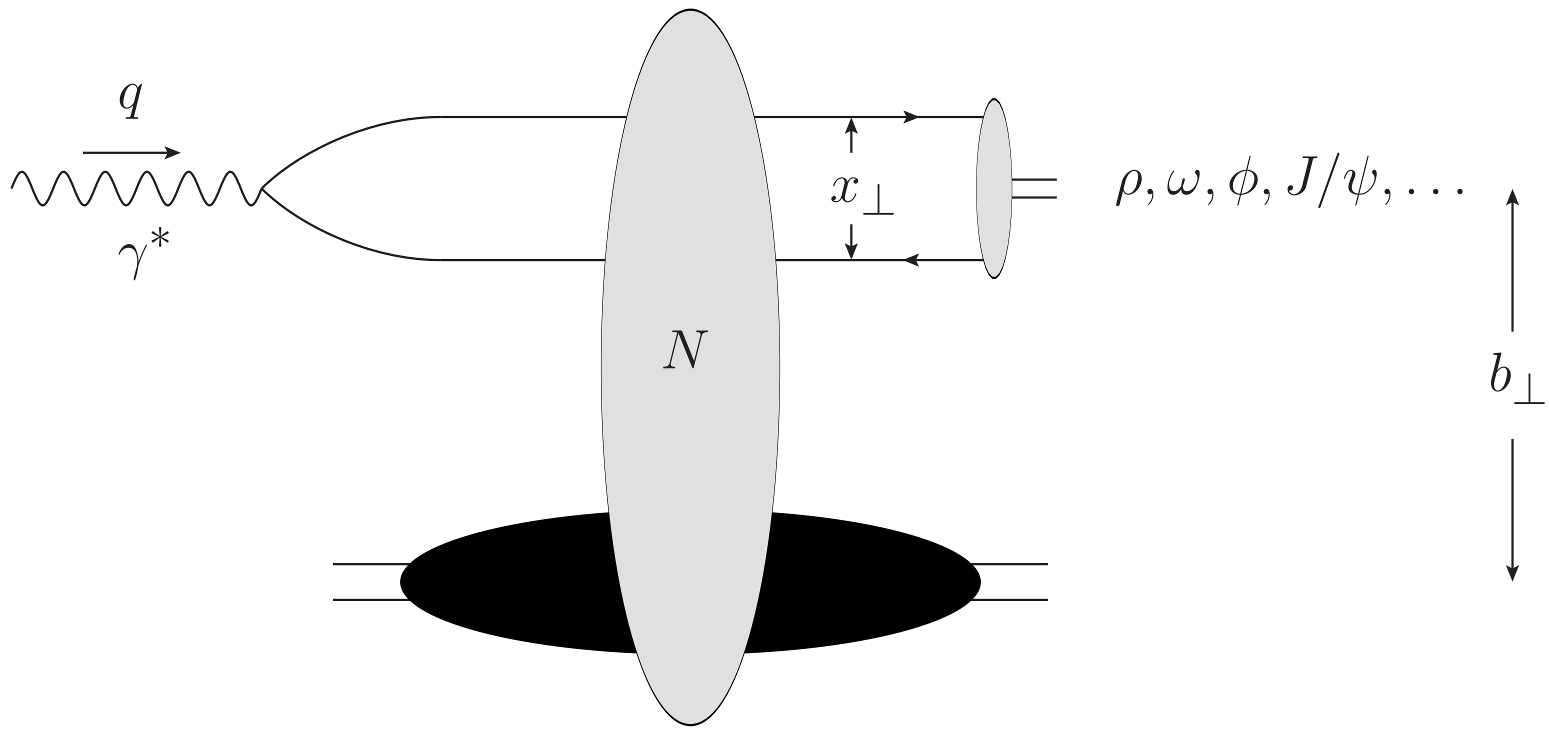

Exclusive VM Production: Probe of Spatial Gluon Distribution

- Differential exclusive VM production cross section is

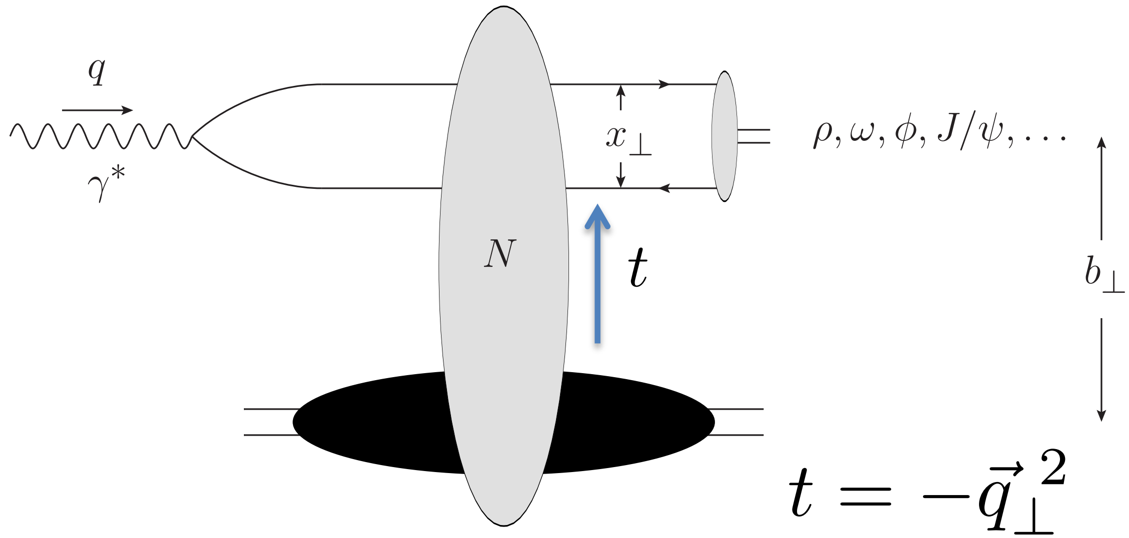

$$\frac{d\sigma^{\gamma^*+A\to V+A}}{dt} = \frac{1}{4\pi}\left|\int d^2b\, e^{-i\,\vec{q}_\perp\cdot\vec{b}_\perp}\, T^{q\bar{q}A}(\hat{s},\vec{b}_\perp)\right|^2$$

- the T-matrix is related to the dipole amplitude N:

$$T^{q\bar{q}A}(\hat{s},\vec{b}_\perp) = i\int\frac{d^2x_\perp}{4\,\pi}\int_0^1\frac{dz}{z\,(1-z)}\;\Psi^{\gamma^*\to q\bar{q}}(\vec{x}_\perp,z)\;N(\vec{x}_\perp,\vec{b}_\perp,Y)\,\Psi^V(\vec{x}_\perp,z)^*$$

Brodsky et al '94, Ryskin '93

- Can study t-dependence of the dσ/dt and look at different mesons **to find the dipole amplitude N(x,b,Y)** (Munier, Stasto, Mueller '01).
- Learn about the **gluon distribution in space**.

Exclusive VM Production as a Probe of Saturation

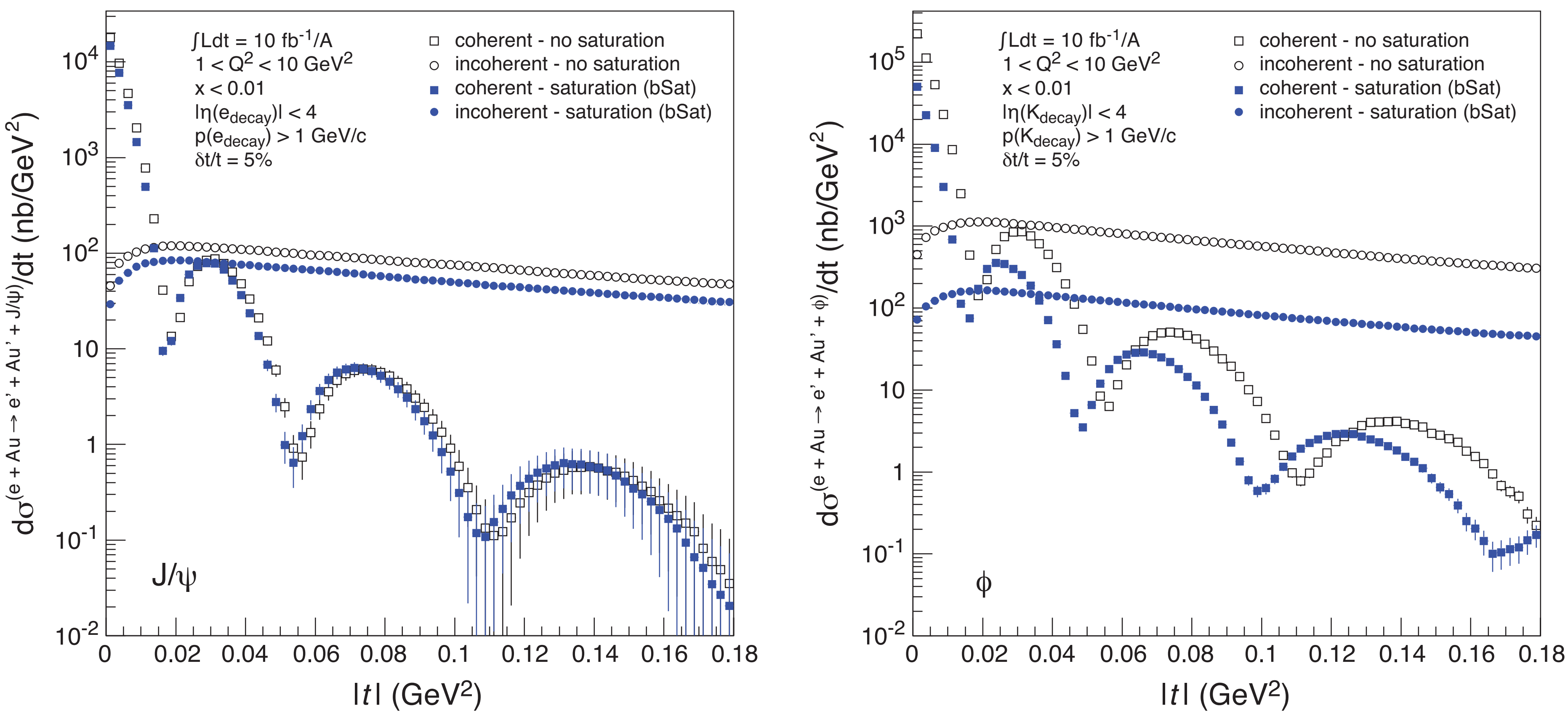

Plots by T. Toll and T. Ullrich using the Sartre event generator (b-Sat (=GBW+b-dep+DGLAP) + WS + MC).

- J/psi is smaller, less sensitive to saturation effects
- Phi meson is larger, more sensitive to saturation effects

Conclusions

- In recent decades we have seen a lot of progress in our understanding of QCD in high energy collisions.
- Multiple rescattering have been summed up at small-x (GGM/MV).
- Non-linear small-x evolution equations have been derived, unitarizing the BFKL evolution, while predicting and quantifying gluon saturation. They led to a lot of successful phenomenology at HERA, RHIC, and LHC, providing possible evidence for gluon saturation (not discussed today).
- EIC will be able to test the predictions of these nonlinear small-x evolution equations and may complete the discovery of parton saturation.

EIC Rings Movie

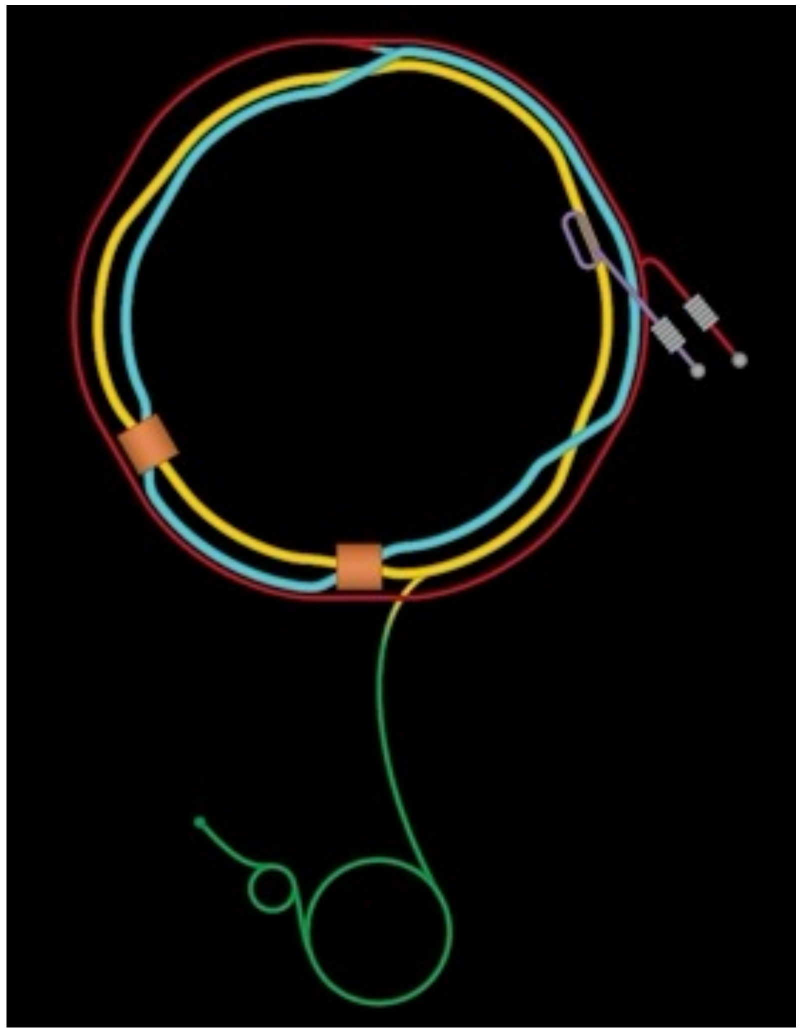

Backup Slides

Black Disk Limit

- Start with basic scattering theory: the final and initial states are related by the S-matrix operator,

$$|\psi_f\rangle = \hat{S}\,|\psi_i\rangle$$

- Write it as $$|\psi_f\rangle = |\psi_i\rangle + \left[\hat{S} - 1\right]\,|\psi_i\rangle$$

- The total cross section is

$$\sigma_{tot} \propto \left|\left[\hat{S} - 1\right]\,|\psi_i\rangle\right|^2 = 2 - S - S^*$$

where the forward matrix element of the S-matrix operator is

$$S = \langle\psi_i|\,\hat{S}\,|\psi_i\rangle$$

and we have used unitarity of the S-matrix

$$\hat{S}\,\hat{S}^\dagger = 1$$

Black Disk Limit

- Now, since $|\psi_f\rangle = |\psi_i\rangle + \left[\hat{S} - 1\right] |\psi_i\rangle$

  the elastic cross section is

$$\sigma_{el} \propto \left|\langle\psi_i| \left[\hat{S} - 1\right] |\psi_i\rangle\right|^2 = |1 - S|^2$$

- The inelastic cross section can be found via

$$\sigma_{tot} = \sigma_{inel} + \sigma_{el}$$

- In the end, for scattering with impact parameter b we write

$$\sigma_{tot} = 2 \int d^2b \, [1 - \mathrm{Re}\, S(b)]$$

$$\sigma_{el} = \int d^2b \, |1 - S(b)|^2$$

$$\sigma_{inel} = \int d^2b \left[1 - |S(b)|^2\right]$$

Unitarity Limit

- Unitarity implies that

$$1 = \langle\psi_i|\,\hat{S}\,\hat{S}^\dagger\,|\psi_i\rangle = \sum_X \langle\psi_i|\,\hat{S}|X\rangle\,\langle X|\hat{S}^\dagger\,|\psi_i\rangle \geq |S|^2$$

- Therefore

$$|S| \leq 1$$

leading to the unitarity bound on the total cross section

$$\sigma_{tot} = 2\int d^2b\,\left[1 - \mathrm{Re}\,S(b)\right] \leq 4\int d^2b = 4\pi R^2$$

- Notice that when S=-1 the inelastic cross section is zero and

$$\sigma_{tot} = 2\int d^2b\,[1 - \mathrm{Re}\,S(b)]$$

$$\sigma_{tot} = 4\pi R^2 = \sigma_{el}$$

$$\sigma_{el} = \int d^2b\,|1 - S(b)|^2$$

This limit is realized in low-energy scattering!

$$\sigma_{inel} = \int d^2b\left[1 - |S(b)|^2\right]$$

Black Disk Limit

- At high energy inelastic processes dominate over elastic. Imposing

$$\sigma_{inel} \geq \sigma_{el}$$

we get

$$\mathrm{Re}\, S \geq 0$$

- The bound on the total cross section is (aka the **black disk limit**)

$$\sigma_{tot} = 2 \int d^2b \,[1 - \mathrm{Re}\, S] \leq 2 \int d^2b = 2\pi R^2$$

- The inelastic and elastic cross sections at the black disk limit are

$$\sigma_{inel} = \sigma_{el} = \pi R^2$$

$$\sigma_{tot} = 2 \int d^2b \,[1 - \mathrm{Re}\, S(b)]$$

$$\sigma_{el} = \int d^2b \,|1 - S(b)|^2$$

$$\sigma_{inel} = \int d^2b \left[1 - |S(b)|^2\right]$$

Notation

- At high energies

$$\mathrm{Im}\, S \approx 0$$

while the dipole amplitude N is the imaginary part of the T-matrix (S=1+iT), such that

$$\mathrm{Re}\, S = 1 - N$$

- The cross sections are

$$\sigma_{tot} = 2 \int d^2 b\, N(x_\perp, b_\perp)$$

$$\sigma_{el} = \int d^2 b\, N^2(x_\perp, b_\perp)$$

$$\sigma_{inel} = \int d^2 b \left[2\, N(x_\perp, b_\perp) - N^2(x_\perp, b_\perp)\right]$$

- We see that N=1 is the black disk limit. Hence $N \leq 1$ as we saw above.

Going Beyond Large N_C: JIMWLK

To do calculations beyond the large-N_C limit on has to use a functional integro-differential equation written by Iancu, Jalilian-Marian, Kovner, Leonidov, McLerran and Weigert (JIMWLK):

$$\frac{\partial Z}{\partial Y} = \alpha_s \left\{ \frac{1}{2} \frac{\delta^2}{\delta \rho(u)\, \delta \rho(v)} \left[Z\, \chi(u, v) \right] - \frac{\delta}{\delta \rho(u)} \left[Z\, \sigma(u) \right] \right\}$$

where the functional Z[ρ] can then be used for obtaining wave function-averaged observables (like Wilson loops for DIS):

$$\langle O \rangle = \int D\rho\, Z[\rho]\, O[\rho]$$

Diffraction in optics

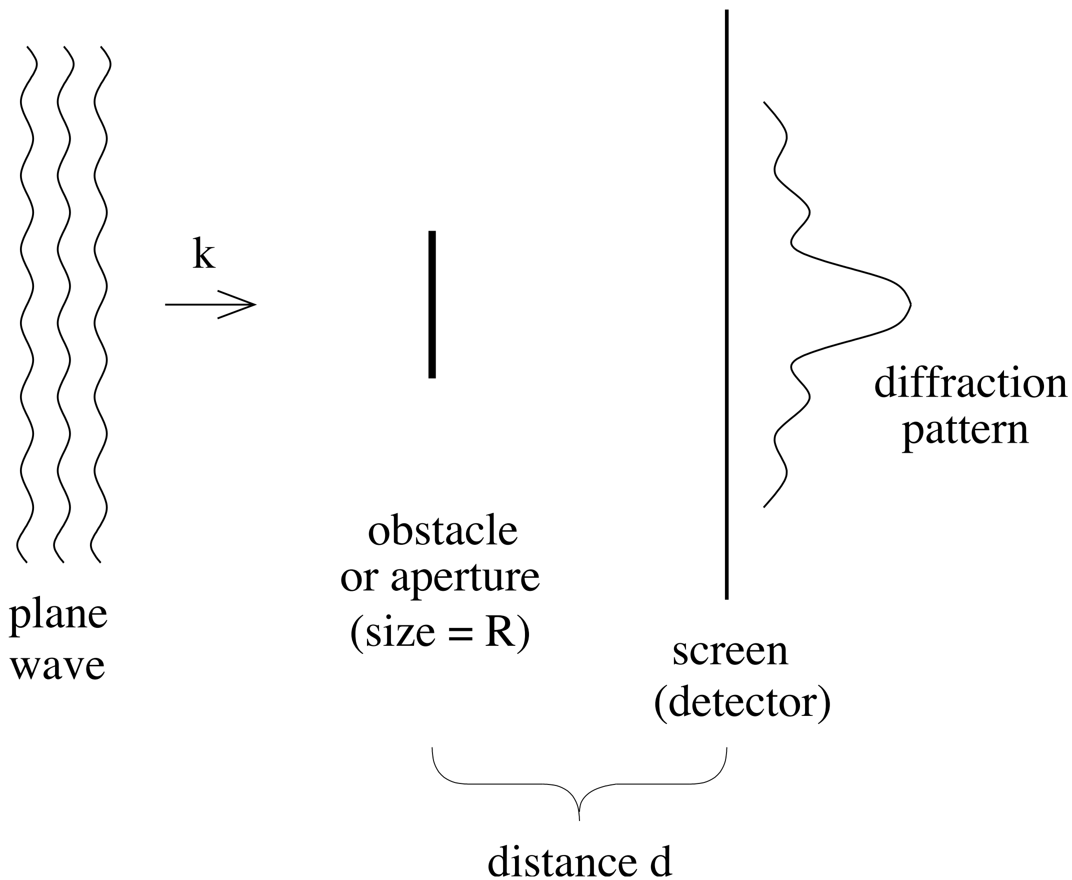

Diffraction pattern contains information about the size R of the obstacle and about the optical “blackness” of the obstacle.
In optics, diffraction pattern is studied as a function of the angle θ. In high energy scattering the diffractive cross sections are plotted as a function of the Mandelstam variable t with $\sqrt{|t|}$ = k sin θ.

Optical Analogy

Diffraction in high energy scattering is not very different from diffraction in optics: both have diffractive maxima and minima. In optics, diffraction pattern is studied as a function of the angle θ. In high-energy scattering the diffractive cross sections are plotted as a function of the Mandelstam variable $t = k \sin \theta$.

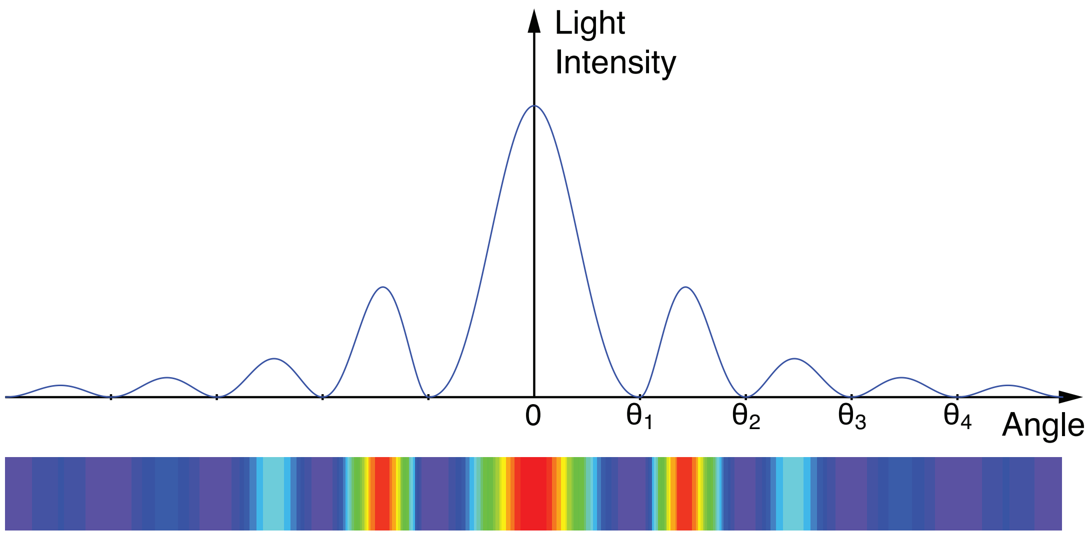

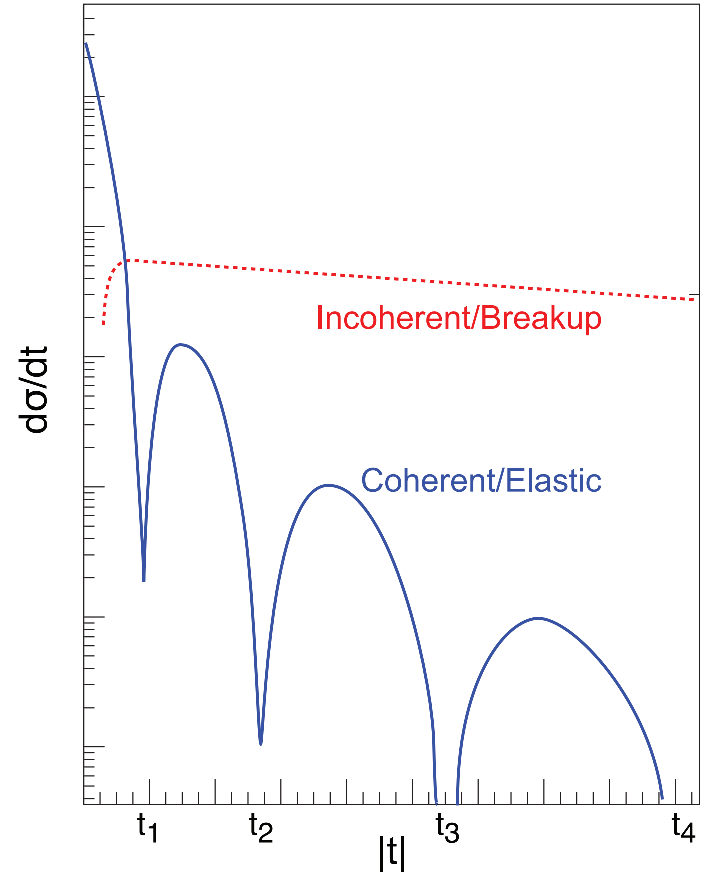

Coherent: target stays intact;

Incoherent: target nucleus breaks up, but nucleons are intact.